ERRATA

SMRP Report #64, Figure B1 should read:

Mosaic of the ITCZ on July 15, 1961 at about 1557 GMT. The cloud mass on the eastern boundary of the picture, labeled W-3, is the western edge of the developing Anna wave.

64

SATELLITE & MESOMETEOROLOGY
RESEARCH PROJECT

Department of the Geophysical Sciences
The University of Chicago

THE TIME CHANGE OF CLOUD FEATURES IN HURRICANE ANNA, 1961, FROM THE EASTERLY WAVE STAGE TO HURRICANE DISSIPATION

by

James E. Arnold

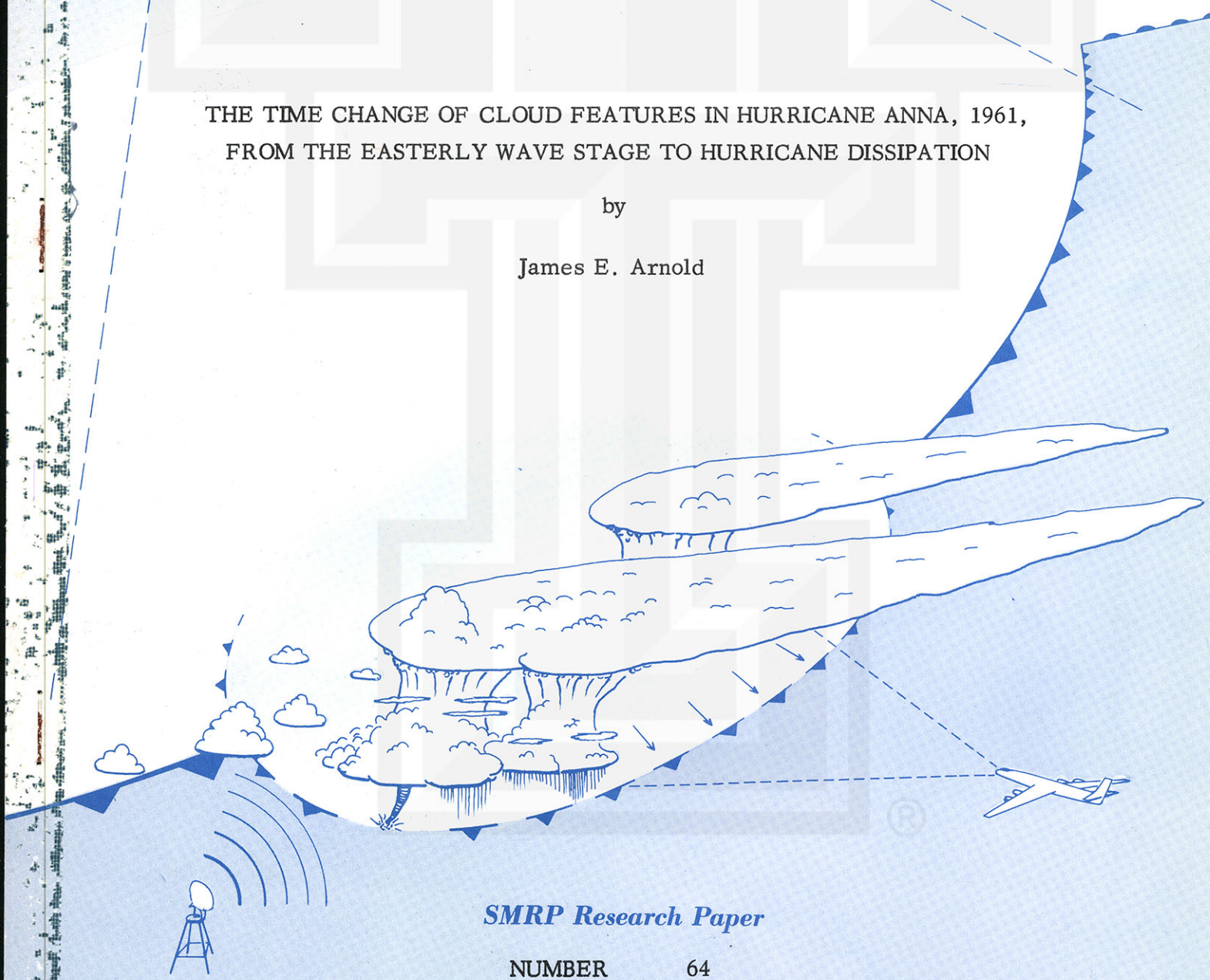

SMRP Research Paper

NUMBER 64

January 1967

MESOMETEOROLOGY PROJECT --- RESEARCH PAPERS

1.* Report on the Chicago Tornado of March 4, 1961 - Rodger A. Brown and Tetsuya Fujita

2.* Index to the NSSP Surface Network - Tetsuya Fujita

3.* Outline of a Technique for Precise Rectification of Satellite Cloud Photographs - Tetsuya Fujita

4.* Horizontal Structure of Mountain Winds - Henry A. Brown

5.* An Investigation of Developmental Processes of the Wake Depression Through Excess Pressure Analysis of Nocturnal Showers - Joseph L. Goldman

6.* Precipitation in the 1960 Flagstaff Mesometeorological Network - Kenneth A. Styber

7.** On a Method of Single- and Dual-Image Photogrammetry of Panoramic Aerial Photographs - Tetsuya Fujita

8. A Review of Researches on Analytical Mesometeorology - Tetsuya Fujita

9. Meteorological Interpretations of Convective Nephsystems Appearing in TIROS Cloud Photographs - Tetsuya Fujita, Toshimitsu Ushijima, William A. Hass, and George T. Dellert, Jr.

10. Study of the Development of Prefrontal Squall-Systems Using NSSP Network Data - Joseph L. Goldman

11. Analysis of Selected Aircraft Data from NSSP Operation, 1962 - Tetsuya Fujita

12. Study of a Long Condensation Trail Photographed by TIROS I - Toshimitsu Ushijima

13. A Technique for Precise Analysis of Satellite Data; Volume I - Photogrammetry (Published as MSL Report No. 14) - Tetsuya Fujita

14. Investigation of a Summer Jet Stream Using TIROS and Aerological Data - Kozo Ninomiya

15. Outline of a Theory and Examples for Precise Analysis of Satellite Radiation Data - Tetsuya Fujita

16. Preliminary Result of Analysis of the Cumulonimbus Cloud of April 21, 1961 - Tetsuya Fujita and James Arnold

17. A Technique for Precise Analysis of Satellite Photographs - Tetsuya Fujita

18. Evaluation of Limb Darkening from TIROS III Radiation Data - S.H.H. Larsen, Tetsuya Fujita, and W.L. Fletcher

19. Synoptic Interpretation of TIROS III Measurements of Infrared Radiation - Finn Pedersen and Tetsuya Fujita

20. TIROS III Measurements of Terrestrial Radiation and Reflected and Scattered Solar Radiation - S.H.H. Larsen, Tetsuya Fujita, and W.L. Fletcher

21. On the Low-level Structure of a Squall Line - Henry A. Brown

22. Thunderstorms and the Low-level Jet - William D. Bonner

23. The Mesoanalysis of an Organized Convective System - Henry A. Brown

24. Preliminary Radar and Photogrammetric Study of the Illinois Tornadoes of April 17 and 22, 1963 - Joseph L. Goldman and Tetsuya Fujita

25. Use of TIROS Pictures for Studies of the Internal Structure of Tropical Storms - Tetsuya Fujita with Rectified Pictures from TIROS I Orbit 125, R/O 128 - Toshimitsu Ushijima

26. An Experiment in the Determination of Geostrophic and Isallobaric Winds from NSSP Pressure Data - William Bonner

27. Proposed Mechanism of Hook Echo Formation - Tetsuya Fujita with a Preliminary Mesosynoptic Analysis of Tornado Cyclone Case of May 26, 1963 - Tetsuya Fujita and Robbi Stuhmer

28. The Decaying Stage of Hurricane Anna of July 1961 as Portrayed by TIROS Cloud Photographs and Infrared Radiation from the Top of the Storm - Tetsuya Fujita and James Arnold

29. A Technique for Precise Analysis of Satellite Data, Volume II - Radiation Analysis, Section 6. Fixed-Position Scanning - Tetsuya Fujita

30. Evaluation of Errors in the Graphical Rectification of Satellite Photographs - Tetsuya Fujita

31. Tables of Scan Nadir and Horizontal Angles - William D. Bonner

32. A Simplified Grid Technique for Determining Scan Lines Generated by the TIROS Scanning Radiometer - James E. Arnold

33. A Study of Cumulus Clouds over the Flagstaff Research Network with the Use of U-2 Photographs - Dorothy L. Bradbury and Tetsuya Fujita

34. The Scanning Printer and Its Application to Detailed Analysis of Satellite Radiation Data - Tetsuya Fujita

35. Synoptic Study of Cold Air Outbreak over the Mediterranean using Satellite Photographs and Radiation Data - Aasmund Rabbe and Tetsuya Fujita

36. Accurate Calibration of Doppler Winds for their use in the Computation of Mesoscale Wind Fields - Tetsuya Fujita

37. Proposed Operation of Intrumented Aircraft for Research on Moisture Fronts and Wake Depressions - Tetsuya Fujita and Dorothy L. Bradbury

38. Statistical and Kinematical Properties of the Low-level Jet Stream - William D. Bonner

39. The Illinois Tornadoes of 17 and 22 April 1963 - Joseph L. Goldman

40. Resolution of the Nimbus High Resolution Infrared Radiometer - Tetsuya Fujita and William R. Bandeen

41. On the Determination of the Exchange Coefficients in Convective Clouds - Rodger A. Brown

* Out of Print
** To be published

(Continued on back cover)

SATELLITE AND MESOMETEOROLOGY RESEARCH PROJECT
Department of the Geophysical Sciences
The University of Chicago

THE TIME CHANGE OF CLOUD FEATURES IN HURRICANE ANNA, 1961, FROM THE EASTERLY WAVE STAGE TO HURRICANE DISSIPATION

by

James E. Arnold

SMRP Research Paper #64
January 1967

The research reported in this paper has been sponsored by the Environmental Science Services Administration under grant Cwb WBG-34.

THE TIME CHANGE OF CLOUD FEATURES IN HURRICANE ANNA, 1961, FROM THE EASTERLY WAVE STAGE TO HURRICANE DISSIPATION[1]

James E. Arnold

Department of the Geophysical Sciences
The University of Chicago
Chicago, Illinois

ABSTRACT

Development of the basic easterly wave that produced Hurricane Anna of 1961 is followed from the time the wave first gave indications of intensifying until the subsequent hurricane dissipated. Using radiation and photographic data obtained from TIROS III during the period from July 16, 1961 to July 25, 1961, combined with standard observations taken from radiosonde stations in the path of the storm, a representative picture of storm behavior is obtained.

It is found that the cloud activity was originally in two adjacent areas with the major cloud activity in the southern portion of the wave and a small cloud area just east of the wave crest. Both are believed to have trailed the wave axis or circulation center. The wave itself developed under a tropical anticyclone with a local anticyclone intensifying over the storm.

Three major cloud bands became apparent almost simultaneously with the formation of the cirrus shield, one of which included the northern or crest cloud. Hurricane intensity was reached within 30 hours of the obscuration of the apparent circulation center and band formation. At maximum intensity the cirrus shield covered the major rain bands leaving an isolated hurricane system as viewed from the satellite. There were also indications of strong convection regions imbedded with-

---

[1] The research reported in this paper has been sponsored by the Environmental Science Services Administration under grant Cwb WBG-34.

in the remnant cirrus shield. A clear region was apparent in front of the storm shield but lay well behind the outer shear line. It is believed that the clear band is more the result of dry air advection than subsidence at the cirrus rim. Although the storm dissipated at the surface, a cirrus cover remained over the depression.

1. Introduction

Examination of cloud structure associated with various phases of hurricane development has provided an insight into the changing cloud organization. Usually, however, a particular storm is not observed continuously throughout its life and a composite of many storms is used to obtain a description of a developing hurricane. In this manner Fett (1964a) has arrived at a model of hurricane development deduced from the associated cloud patterns. He found that basically the development in the cloud pattern associated with the developing system could be subdivided into four stages ranging from an elongated cloud mass along the wave axis to that of the well-developed cirrus shield over the actual hurricane.

Shiroma and Sadler (1965) in a study of typhoons found that the early stages of development were not associated with a recognizable vortex in the cloud field, but, in the case of vortices imbedded in the low level trough, the initial cloud system was situated on the south side of the trough. It was also observed that the predominant cloud system was east of the surface vortex center when the system had developed from aloft downward. It has also been observed by Sadler (1964) and Fett (1964b) that, as the storm becomes mature, it is sometimes surrounded by a clear area termed an annular ring.

Hurricane Anna has been the subject of several investigations, all dealing with selected portions of her life. Fritz (1962) has described cloud features associated with the early development stage of the vortex and suggested that it developed from an easterly wave which traveled from the coast of Africa into the western Atlantic. Fujita and Arnold (1964) examined the early wave stage of Anna and showed that it originated from a pre-existing system coming from Africa. In a related study Arnold (1966) examined developing cloud patterns associated with easterly waves in the Atlantic contemporary with the wave that developed into Hurricane Anna. It was found that most of the waves had a cloud pattern which was first simply an area of increased activity along the ITCZ, and then,as the wave developed, added a second characteristic

cloud northeast of the assumed wave axis. This later cloud pattern consisted of a large base cloud, i.e., that cloud or cloud group that previously existed as a bulge in the ITCZ and a smaller crest cloud located north of the base cloud and just to the rear of the wave crest. The early wave stage of Anna was similar to other waves in the train in cloud distribution with the exception that the wave that developed into Hurricane Anna was relatively intense through its entire Atlantic crossing compared to other waves in the wave train.

This study examines the development of Hurricane Anna from the time the wave began to intensify in the mid-Atlantic to its dissipation off the coast of Mexico. The satellite photographs and radiation data are used in conjunction with standard radiosonde observations taken along the path of the storm to describe the life cycle in terms of cloud development. The radiation data were taken from the original analog traces to obtain contour features of the cloud tops thus enabling the orientation of individual cloud bands in the cirrus to be determined. Cloud top temperatures have been corrected for instrument degradation but not for viewing angle effects. It may be assumed that the temperatures are relatively accurate when a large cloud area is observed, but, because of scan spot size, temperatures of small towers will be in error as part of the cloud wall is also sensed. In addition, low cloud tops, as well as ocean surfaces, will have a temperature error due to radiation absorption by the intervening moisture in the lower atmosphere.

Because synoptic data were sparce at best, maps of streamlines have not been included in this study. It is felt that such maps would only add to the number of assumptions made about the developing storm. For the reader desiring an idea of the circulation fields connected with various satellite photographs of hurricane development, articles by Shiroma and Sadler (1965), and Merritt (1965) have excellent examples.

2. Background History

Synoptically speaking, the wave which developed into Hurricane Anna originated over the African continent and traveled westward in the general flow. The wave came into conjunction with at least one southward-extending subtropical trough off the coast of Africa and possibly with a second in the central Atlantic. For the most part during the early stage of the storm, the Sahara Anticyclone and the Atlantic Anticyclone were well-developed and deep easterly flow existed across the tropical Atlantic. Wave development, as well as storm intensification, took place under a broad tropical high

which certainly contributed to the upper ventilation of the system.

As the westward-moving storm evolved and the high pressure dome over the developing wave intensified, the southern end of an eastward-moving subtropical trough was sheared off and pushed westward in front of the storm. Initially, on July 17, the distance between the trough and the storm center was on the order of 13 degrees of longitude; however, as the storm aged the distance decreased to approximately 5 degrees by July 23, as can be seen in Fig. 1. The closer distance between the storm and the shear line corresponded to the distance the cirrus coverage extended in the forward quadrant of the storm.

The wave that produced Hurricane Anna was just one of a series of waves traversing the Atlantic at that time and Erickson (1963) noted a similar wave series present during August and September of the same year indicating that the situation of multiple waves was not unique. Historically speaking, it seems that at least three of the hurricanes for the 1961 season (Anna, Debbie, and Esther) were associated with waves that passed from Africa into the Atlantic. In the case of the Anna wave, as with other waves of the period, existence and movement was along the ITCZ since an almost continuous cloud band was present across the Atlantic. The convergence zone cloud pattern was well-defined during the early period and at least one band of the convergence zone passed through a portion of the active wave until the disturbance reached the western Atlantic.

On July 12, the first day of TIROS coverage, the wave consisted of two cloud areas with a considerable amount of high cloud cover.[1] It is very likely that the high clouds present were cirrus associated with the convective towers in the wave. Almost coincident with the passing of the wave into the Atlantic was the conjunction of the easterly wave with a high level subtropical trough. The effect of the conjunction seems to have been a great increase in cloud cover over the wave activity and an almost complete halt in the westward progress of the wave for a short period of time. Although the cloud cover increased greatly, the two areas of cloud activity that had been present on the previous day remained. The northern portion of cloud activity increased greatly in area while the activity associated with the southern cloud area became semi-circular in appearance. Satellite observation of the system on July 14 showed that it had moved westward about six degrees along the convergence zone. The two areas of cloud activity had been retained; however, the overall cloud area had decreased

---

[1] Radiation maps (8-12 μ) for July 12, 13, and 14, 1961 are shown in Appendix A.

considerably. During the first three days of observation the coldest cloud top temperatures did not change appreciably and were usually colder than -50C. By July 16 the wave had reached the mid-Atlantic (39W) and had decreased in cloud area while cloud top temperatures had warmed greatly (to -32C) from maximum intensity on July 13.

3. The Observed Hurricane Life Cycle

The mid-Atlantic position of the wave marks the end of the general dissipation observed from its maximum intensity on July 13. The radiation pattern for July 16 (Fig. 2) shows that the system is still composed of two cloud areas and probably indicates that a well-developed wave exists at the surface. The southern cloud mass is connected to the main ITCZ as was the case earlier in its life. The cloud areas themselves seem to be composed of several regions of strong convective activity covered by a cirrus deck as can be seen in Fig. 3. Fritz (1962) has previously suggested that the actual center of the system lies west of the cloud mass and later developments in the cloud field seem to support this concept.

By July 17, as observed by the TIROS camera and radiometer, the cloud pattern shown in Figs. 4 and 5 has undergone a development in both area and vertical extent. Radiative cloud top temperatures have lowered from a minimum of -32C on July 16 to -51C on July 17. The horizontal extent of the cloud coverage has increased considerably in the northern or crest cloud while the cloud mass to the south has developed vertically. Ahead of the crest cloud, a streamer can be seen in the radiation data which is probably associated with cirrus streaming off the base cloud. Faint indications of this streamer are apparent in the photograph; however, its proximity to the picture horizon makes definite identification difficult. On the other hand, the cloud band trailing from the crest cloud shows up well in the photograph shown in Fig. 4 but can only be detected as a faint distortion in the isotherm pattern in the radiation map (Fig. 5) at the same time. In fact, a comparison between the band as it appeared in the radiation data on July 16 (Fig. 2) and as it appeared on July 17 (Fig. 4) shows that it was more pronounced on the earlier day. The southern cloud band entering the base cloud is still present on July 17 as can be seen in both the radiation and photographic data.

A speculative interpretation of the radiation and photographic information for July 17 is that the wave is still in an open stage with strong convergence taking place in the crest of the wave and in the pressure trough, predominately behind the

wave axis. It is difficult to determine where the area of lowest pressure is at this time; however, assuming that the wave axis was ahead of the cloud system on July 16, it seems likely the same is true for July 17.

The satellite coverage of the storm on July 18 is restricted to the westward half in both the radiation and photographic data. From continuity, however, most of the features present in the data on July 17 can be located on July 18. The eastward-extending cloud band present on July 17 can not be seen in the photograph[2] over the storm but can be detected in the photograph coverage in the preceding orbit. The strong distinction between the base and crest clouds does not seem to be present to the degree that existed on the previous day. As can be seen in Fig. 6, the base cloud has developed an almost semicircular nature, very similar to that present on July 13, with the crest cloud connected to it at the westward end. Cloud top temperatures are almost uniform in both the crest and base cloud with minimum temperatures of about -42C. Ahead of the base cloud, a third cloud system has developed with a relatively warm region between the new cloud system and the base cloud. Assuming that the wave axis has been ahead of the cloud system in the past, this could be the beginning of cloud development west of the actual circulation center. This being the case, we still have a storm system with an open eye or circulation center but with a significant development in the cloud pattern. It should be recalled that this is the third day of development from the basic bimodal system. Cloud streamers present in the photograph of the system at this time indicate that the storm system is under southeasterly winds which agrees well with the synoptic analysis shown in Fig. 7.

Transistion of the developing hurricane from two cloud areas with an open circulation center to a cirrus covered center has occurred by observation time on July 19. Although no photographic observation was made, the infrared data give an excellent portrayal of the storm. At this time, the cirrus canopy covers what must have been the base cloud, the western-eye-wall cloud, and the eye itself. As can be seen in Fig. 8, the crest cloud is still prominent and relatively isolated from the cirrus canopy. As will be seen later, the canopy gradually expands to cover the outlying cloud

---

[2] TIROS III photographs for July 16-18, 20-23, and 25 of the developing and mature hurricane are shown in sequence in Appendix B. A photographic composite is shown for the area that probably covers the wave on July 15.

system. From the radiation maps, it can be seen that the cloud top temperatures were on the order of -46C on July 18 but had decreased to -60C by July 19. The large decrease in cloud top temperatures can probably be attributed to the smaller area of cloud intercepted by the radiation sensor on the 19th than on the 18th because of the oblique angle at which the storm was viewed on the 18th as much as to an actual increase in cloud heights.

The irregularity in the isotherm pattern on July 19 suggests that cloud bands were radiating from the storm center at the high cloud level. In addition, two bands seem to be associated with the low level flow. In the case of the low level bands, both are in the northern part of the cloud field, one being a remnant of the existing long cloud trail extending from the crest cloud on previous days. The second band coincides with a line-group of clouds present in the photographs of the system on July 20.

At high levels the cloud streamers are being swept southward from the main cloud mass in the anticyclone over the storm. Although it is not readily apparent in the radiation pattern on July 19, the first major cirrus cloud band (A) is developing and now extends from the storm center over the crest cloud. A second major cloud band (B) extends beyond the edge of the cirrus shield toward the south.

A tongue of warm air has become apparent in the radiation pattern west of the cloud system associated with the developing hurricane. The tongue, which is even more pronounced when a broad area is viewed, does not seem to be the result of an actual warming of the air but could be due to drying which would permit more outgoing radiation to be intercepted by the satellite radiometer. Although this hypothesis is not supported to any great extent at the time the storm passes the raob station at Chaguaramas, its probability seems likely in view of cloud band orientation north of the storm.

A time cross-section depicting the developing system as it goes by the raob station at Chaguaramas early on July 20 (Fig. 9) indicates that the system had a warm core with most of the heating occurring above 400 mb. Coupled with the maximum heating aloft is a circulation center and a well-pronounced maximum in the humidity field. The presence of both a cyclonic and an anticyclonic circulation aloft in addition to the heat and moisture maximum suggests that the system is developing from high levels downward. Maximum warming in the temperature field behind the wave axis is probably a product of the earlier convection maximum to the rear of the wave axis. It is interesting to note that the humidity field in front of the storm is still characteristic of the easterly wave and does not exhibit the strong drying at low levels that appears later in the life of the storm. The wave axis for the most part is vertical. The cloud bands in the radiation map for July 19 are not reflected in the cross section; however, it is

suspected that the only band that extends over the station is of cirrus nature and probably would not be reflected in the coarse data field.

Transisition from the tropical storm stage to that of a hurricane occurred on what can be called the fourth day of intensification (July 20). The storm evolved rapidly at the surface going from a weak disturbance with winds probably less than 20 kt on July 19 to a full hurricane with a minimum pressure of 992 mb and maximum winds of 90 kt on July 20. Coverage of the storm at this time was achieved by combining two orbits of radiation data to produce Fig. 10. The gap in data resulted because areas of radiation coverage did not overlap from orbit to orbit. In spite of this, the radiation map is probably a representative picture of the cloud top structure.

A comparison between the radiation pictures on July 19 and July 20 reveals that the crest cloud has disappeared altogether by the 20th. At the same time it can be seen that the shield has not greatly expanded in the 24 hr period with the exception of the elongation along the cloud bands. Band A, which includes the crest cloud, has become more a true cloud band in relation to the central storm circulation at high levels rather than a low level convergence axis to the rear of the storm. Although band A must have a considerable amount of cirrus near the storm, the cirrus quickly fades and the actual radiation band orientation on the eastern end seems to be governed to a great extent by a low-level cloud band just north of the main band A.

The cloud band B has become much more prominent and a new band C has developed forward of the storm. Because of its shape and cold core, C must have some strong convective activity taking place within it. The rear band (B), although prominent, has a relatively flat temperature gradient across the top and a uniform appearance in the photograph indicating that it is composed of high clouds. (Appendix B)

The cirrus shield itself is composed of two individual cold domes within the shield boundary, which now appear to surround the eye of the storm. A rough comparison with radar data taken six hours earlier indicated that the domes themselves as well as cloud band C are nearly coincident with major spiral bands in the radar data. In fact, at this time there is some ambiguity whether cloud band C and A overlay the same radar spiral band. An additional satellite-observed cloud band which coincides with the radar data occurs in the northwestward extension of cloud band C. Under the cloud band a weak line of radar echoes exists that crosses the main spiral bands at an angle of approximately 60°. Since it is reasonably certain that there was cirrus

coverage over the echoes, a seeding process seems likely from the high levels into the lower region.

In Fig. 11 a forward cloud band has been sketched in subjectively, primarily on the basis of the indicated cooling observed in the lower 3 km (1200 GMT, July 20). This cooling is assumed to be the result of precipitation associated with the band. It is apparent that the atmosphere is cooling about the storm while the warm core is expanding vertically from that which had existed as the storm passed over Chaguaramas. The outflow is slowly developing; however, it still corresponds closely to the horizontal area of cirrus coverage as inferred from the radiation data.[3]

One of the most prominent atmospheric features that has developed by this time is the minimum in the humidity field at low levels in front of the storm. This minimum occurs well behind the outer shear line mentioned previously. Although the dry area is close to the actual cirrus boundary or shield edge, it is difficult to make a direct connection between the two. As can be seen, relatively strong cooling is taking place through the entire column in the area both in front of and behind the storm. In view of this it seems unlikely that any appreciably deep subsidence could be taking place. On the other hand, dry air being advected around the front of the storm from higher latitudes would conform with both the indications of such an occurrence in the synoptic data and the warm tongue present in front of the storm in the radiation map.

By July 21, the fifth day of the observed life cycle, the cirrus shield has become well-developed with three cirrus covered bands easily identifiable. The cirrus shield itself has no definite boundary as yet with the edges slowly fading into finger-like extrusions beyond the hard core cirrus. At the surface the central pressure has reached 981 mb with maximum winds over 100 kt.

The cloud bands that have been present since July 19 are easily identifiable in both the photograph (Appendix B) and the radiation data covering the storm on July 21. In the radiation data presented in Fig. 12, band A can be seen as a high cloud streamer extending away from the storm to the east. As opposed to the previous day when the

---

[3] The presence of the developing wave under the tropical anticyclone creates a problem in determining the forward extent of the actual outflow associated with the developing system. While a marked shear line seems to be associated with the rear edge of the outflow which coincides with the apparent cirrus coverage, the shear line in front of the storm does not seem to be as much a product of the outflow as of the overall synoptic situation.

radiation cloud band was composed of both the low-level cloud area to the north of the storm and the cirrus streamer, the band now appears to be entirely made up of high clouds. Apparently the cloud tail that was present on earlier days in the low cloud field extending from the crest cloud has its counterpart aloft on July 21, but, because of orbital coverage, its eastward extension is not known. Cloud band B can be seen in the radiation data as an elongation of the temperature contours and in the photograph as first an elongation of the cirrus shield and further out as a thin cirrus veil. The large cloud mass at the end of the B cloud band is associated with orographic convection over the mountains in Venezuela. Cloud band C is present as an elongation in the radiation data contours and an extension of the high cloud shield visible in the photograph. It will be recalled that because of a small gap in the radiation coverage over the storm on July 20, bands A and C could not be clearly separated. On July 21, the satellite coverage shows that they are two individual bands. Cloud band A, however, is the more intense of the two and coincides with the strongest radar band observed by the aircraft. Several other smaller cloud bands or wisps can be seen in the photograph but do not appear to be organized into any definite bands or band groups as was the case for the three bands that seemed to maintain their identity for long periods of time.

In the cirrus shield itself, there appears to be good association between top features present in the radiation data on July 20 and those present on July 21. If coldest cloud tops can be associated with the strongest convection activity, the most vigorous convection on July 20 and July 21 has been taking place to the rear of the storm center in the vicinity of 20-2 and 21-2 in Figs. 10 and 12. Other areas of intense convection seem to correspond in a similar manner, i.e., 20-1 corresponds to 21-1 and 20-3 corresponds to 21-3 in Figs. 10 and 12.

Six days after intensification began (July 22), the storm reached maximum intensity with maximum observed winds near 110 kt and a minimum surface pressure of 976 mb. At this time the hurricane was in the mid-Caribbean and exhibited a well-developed cirrus shield as can be seen in Fig. 13. Although there are thin cirrus clouds beyond the hard core cirrus within the cirrus canopy, mainly to the north of the storm, a definite boundary is present about much of the storm. The spiral cloud configuration within the cirrus shield is not as apparent in the photograph taken on July 22 (Fig. 13) as it was in the photograph taken on the previous day; however, it remains distinct in the radiation map of the storm top in Fig. 14.

For reference purposes, the high level circulation over the storm and adjacent area can be seen in Fig. 15, which depicts the 200 mb surface at 1200Z on July 22. The 200 mb level has become dominated by the storm-associated system, which, at this time, consists of a high pressure dome over the hurricane followed by an isolated dome a few degrees behind the hurricane center. An anticyclone trailing the storm is well-developed and seems to be responsible for the large clear ocean area observed to the rear of the storm in the photograph shown in Fig. 14. The trough or shear line that has existed in front of the storm since July 17 is slowly coming closer to the storm, or more specifically, the storm is moving closer to the shear line and on July 22 is about 8 degrees from it in the forward quadrant. The line itself is wrapped about the western and northern part of the storm with the zone of maximum winds usually noted to the north of many developing hurricanes. It is also in this region of maximum winds that a cirrus plume or veil that is present for the remainder of the life of the storm has begun to develop. Well behind the storm lies a subtropical trough which will eventually contribute to the formation of the trailing vortex observed later in the life of the storm.

The time cross-section from Swan Island (Fig. 16) provides an opportunity to examine some of the features associated with the passing hurricane in more detail. As can be seen, the circulation in the high pressure dome over the storm is well-defined in the cross section. The shear line at 200 mb that has been at too great a distance to be observed in the two previous cross sections is now relatively close to the storm center. From the temperature anomalies and the drying ahead of the storm, it seems quite possible that significant subsidence occurs just ahead of the line. Approximately under or slightly behind the high level outer shear line is a supplemental shear line; however, photographic evidence of any associated activity on July 22 is obscured near the picture horizons.

The edge of the cirrus shield is clearly associated with a strong warming through a shallow depth in the vertical cross-section as it passes over the station and the line or band that has slowly become more apparent in the preceding cross-sections is well-defined below it. There is a second shallow area of warming at the rear of the cirrus shield suggesting that there is probably a shallow area of warming around much of the shield of the storm. It is interesting to note, however, that in both cases the warming is only present in the immediate vicinity of the cirrus edge and does not extend to any appreciable depth. The dry region, at 700 to 300 mb, slightly ahead of the cirrus edge is well-pronounced at this time but is still associated with a region of cooling. It should also

be pointed out that the dry region in the cross section continues to coincide with the warm (dry) tongue observed ahead of the storm in the radiation map.

The cloud shield on July 23 has undergone a continued expansion as can be seen in the radiation map shown in Fig. 17. The tendency of the shield to become more asymmetric toward the right hand quadrant has increased and what must be a cirrus veil has extended along the axis of the maximum wind. At the surface the storm has undergone a decrease in intensity with maximum winds of about 90 kt and a minimum central pressure of 982 mb.

A decrease of storm intensity continued through July 24, with no useable coverage, and by July 25 (the 8th day after the storm began to intensify and the third day after dissipation set in) the shield began to break up and contained several smaller cold domes in the vicinity of the remnant storm at the surface, as can be seen in Figs. 18 and 19. A cirrus veil that began to extend along the region of maximum winds earlier remains the main indication of the previous spiral structure of the storm.

As for the cloud shield itself, expansion for July 21, 22, and 23, when good photographic coverage is available, can be seen to follow a definite pattern as shown in Fig. 20. On July 21 the shield had much of the characteristics of the earlier periods after shield formation with the spiral bands well-defined. On July 22 the shield had expanded over the individual bands leaving an almost uniform shield visible from the satellite. By July 23 the asymmetric structure of the cloud shield is very apparent with its main elongation from the storm center along the maximum wind axis to the north and over the earlier principal cloud band A. After July 23 the shield structure continued to elongate and gradually broke up.

4. The Pre-Hurricane Clear or Annular Zone

Lately, increasing attention has been given to the clear zone sometimes present about portions of the cirrus shield associated with the mature hurricane. As has been mentioned, both Fett (1964b) and Sadler (1964) have noted this clear or "annular zone" present about the mature hurricane or typhoon and it has been proposed that it is the result of subsidence along the outer shear line at the cirrus edge. Reap (1966) has used such a hypothesis as the basis of a study in which good agreement was found between the outer cirrus edge, the outer shear line and drying and an absence of low clouds in front of Hurricane Dora. Fujita et. al. (1966), on the other hand, treat the clear or annular zone as a convergence product associated with the development

and maintenance of an outer convection line and located between the convection line itself and the inner cirrus shield. In the latter case subsidence in the clear zone needs not extend to deep layers. Thus, drying initiated from deep subsidence and low-level convection suppression is not necessarily inherent in the model.

In the case of Hurricane Anna, it has been pointed out that the usual clear zone is present at the time the storm is at maximum intensity, so it is informative to examine factors which could have contributed to its presence. A brief outline of features present at the time the clear zone is observed is convenient. From photographic and synoptic observations the following can be determined;

1. A clear band is present about the forward half of the storm and to a very faint degree in the rear.
2. In the satellite photographs, hard cloud spots seem to be present in the vicinity of the forward cirrus edge, supported to some extent by radiation data.
3. A thin band or line of clouds is present for a short distance on the leading edge of the clear area in the left front quadrant of the storm (Fig. 13).
4. A broad cloud area exists ahead of the apparent annular zone.
5. From the time cross-section at Swan Island it can be seen that a shallow area of warming has occurred at the cirrus edge as the storm passed the station.
6. Beneath the cirrus rim in the Swan Island cross section, a shear line is present which is assumed to correspond to a convection line.
7. Ahead of the cirrus rim of the storm, there is a dry region extending upward from 850 mb.

Combining all the individual features, a net picture is found similar to that which has been described by Fujita et. al. (1966) in the vicinity of the outer convection band. The hard cloud spots at the cirrus rim could be the tops of vigorous convection associated with the outer convection band and seem to be reflected in the time cross-section for Swan Island. Since the time interval of observation at Swan Island is relatively large, it is difficult to position the warming at the cirrus rim as ahead of or behind the convection line, but, in either case, it does not extend to any great depth. The dry air, on the other hand, extends through a deep layer but is associated with a region of net cooling. In the cloud field in front of the storm the broad cloudy region previously mentioned overlays the landmass on Nicaragua and Honduras and is probably cumulus

associated with diurnal heating and the general orographic effect. This leaves the clear area itself and the thin cloud band to be explained. The cloud band may have had an analogous counterpart to the rear of the storm on the previous day. Inspection of film taken on the reconnaissance flight of July 21 showed that as the aircraft exited at the rear of the storm, cloud bands were present, imbedded in a broad region otherwise void of low clouds. Between the last area of vigorous convection, 32 miles behind the cirrus edge, and the edge of the edge of the cirrus there was one small band of cumulus activity. The remainder of the area under the shield was characterized by thin wisps of clouds at flight level (about 10,000 ft) and predominately clear air. The middle cloud wisps continued well beyond the cirrus edge and ended just before a second broad cloud band was encountered 15 miles from the cirrus edge. Approximately 30 miles beyond the cirrus edge a third region of low clouds was encountered which loosely gives cloud bands at intervals of 26 and 54 miles from the cirrus edge. The symmetry of the cloud bands observed both from the aircraft on July 21 and the satellite on July 22 seems to suggest flow instability at low levels rather than actual suppression of cloud features from above, i.e., subsidence.

Thus, the dry or clear area in front of the storm could very well be simply the result of dry air advection from northern latitudes about the storm circulation. Broad low-level inflow from higher latitudes can be implied from the organization of cloud bands in the early life of the developing hurricane.

It should be pointed out, however, that Hurricane Anna is under a somewhat different synoptic situation than other hurricanes in which the drying at the cirrus edge has been observed. It will be recalled that the shear line that precedes this storm is still well in front of the cirrus edge at the time the clear zone is observed. In many other cases, the hurricane has been further north and the shear line and the cirrus edge coincided. If such had been the case here, it is very likely that the deep drying associated with the cirrus edge and the outer shear line would have occurred here to produce a feature like an annular ring.

5. Discussion of the Hurricane

The development of the basic easterly wave that evolved into Hurricane Anna seemed to follow the basic pattern set down by Riehl (1954) and many of the details described by Yanai (1961). General cloud patterns were similar to those described by Fett (1964a) and Sadler (1964) for individual cases.

Hurricane Anna, as an incipient wave off the west coast of Africa, had a bimodal cloud pattern which consisted of a base cloud in the vicinity of the pressure minimum associated with the ITCZ and a smaller crest cloud located northeast of the base cloud. From the intensity of the cloud system, both the base and crest cloud, when the storm was first detected off the coast of Africa, the wave was probably well-developed when it became oceanic. The general cloud activity associated with the wave decreased in intensity as the wave moved westward into the central Atlantic and probably reached a minimum on July 15 or 16. Ambiguity results from doubtful coverage on July 15. In any case, if the wave were in existence on July 15 it was of very weak intensity. When the wave was observed on July 16 extensive cloud activity was found in the base cloud which apparently consisted of numerous convection centers covered by a thin cirrus shield. The crest cloud was well-defined to the northeast of the base cloud and apparently had at least a short tail or cirrus streamer extending eastward. The eastward-extending streamer at what appears to be the cirrus level implies that the tropical high was situated south of the system as was inferred from synoptic maps covering the area. Because of the lack of surface data it is difficult to say anything definite about the degree of organization at the surface; however, the wave is probably still open. There are faint indications of circulation in the low cloud field in front of the base cloud but not to the degree that usually exists for a surface vortex. Assuming this is the wave axis, however, almost all the major activity is taking place behind the axis with the predominant part of it in the base cloud which at this time must be in the equatorial trough. There seems to be a significant number of cumulus towers imbedded within the cirrus of the base cloud indicating that a considerable amount of heat and moisture must be added to the upper levels of the atmosphere.

Continued intensification of the wave was reflected by an increase of cloud cover over the base and crest cloud. The increase in the cloud cover over the crest cloud was especially large and in the early stage provided the greatest departure from the usual wave cloud areas observed in the Atlantic at this time. Accompaning the increase in cloud top area on July 17 was a significant decrease in cloud top temperature, from just less than -30C to less than -50C. Both regions of activity, however, remained separate through the early development stages with the base cloud consistently connecting with a cloud band which can be assumed to be at least a portion of the main intertropical convergence zone. The intensity of the cloud streamer off the crest cloud increased more in organization and length than in vertical development. In fact, except for a

small amount of cirrus near the crest cloud, the streamer or tail seemed to be made up completely of low clouds. On July 16 and 17 there were indications of strong convection capped with extensive cirrus but it was not until July 18, the third day after intensification began, that any indications of strong convection became apparent to the west of the base cloud and the suspected circulation center. On July 18, however, a cloud area with cold tops (-40C) had appeared to the west of the base cloud with additional indications of cirrus south of the suspected circulation center. The organization sometimes seen in the low cloud field in the vicinity of the circulation center was never observed, suggesting that the main storm organization took place aloft at this time. Support to this concept is given by the raob data from Chaguaramas where the most intense circulation was taking place above 400 mb.

Between July 18 and July 19 the cirrus canopy had formed over the storm center but did not cover the crest cloud. During this time the circulation at the surface probably became more organized but did not develop appreciably high winds. The time the storm actually changed from cold core to warm core is doubtful, but the transition had taken place by the time the storm passed Chaguaramas early on July 20. It seems likely that the transition could have occurred about the time the cirrus canopy developed, sometime early on July 19.

According to the Navy Reconnaissance data (1962), Anna became a hurricane late on July 20, only a little over a day from the time of assumed warm-core creation. Apparently the maximum winds increased very rapidly since at the time of satellite observation on July 19 there were no reported winds greater than 18 or 20 kt in the region of storm development.

Except for the cloud band entering the crest cloud, organization of major cloud bands in the satellite photographs and radiation data did not occur until the apparent circulation center was covered by cirrus. After the cirrus canopy formed, three cloud bands could be detected. The most intense cloud band during the mature portion of the life of the hurricane passed through the position of the crest cloud and through the right front quadrant of the storm. This cloud band was also associated with the most intense radar spiral band. A second cloud band passed through the rear quadrant of the storm and a third radiated out from the left front storm quadrant. In addition to the main cloud bands observed at the cirrus level, organization of low cloud groups into broad cloud bands could be detected, especially in the area north or in the right half of the storm. By the time the storm had reached maximum intensity the connection it had

with the convergence zone cloud system had disappeared.

As the storm increased in intensity the cirrus canopy gradually covered the cloud bands mentioned above, and, although the photographic presence of the cloud bands was hard to determine, they were still apparent in the radiation data. The cloud bands discussed here seem to be what Fujita terms the inner convection bands and correspond well with similar cloud bands dramatically illustrated in some of the typhoon pictures taken by the NIMBUS system (Allison and Nicholas, 1964). On July 22, the day of maximum storm intensity, there are faint indications that convection towers associated with the "outer convection band" are present along the cirrus rim. A clear zone between the outer convection band and the hard inner cirrus shield seems to be absent in this case.

Since major cloud bands did not appear until cirrus had covered the entire central portion of the storm, a feature which also coincided with the start of the rapid intensification of the storm, a connection between the two processes seems likely. Along this line Fujita et. al. (1966) have proposed that convective bands within the storm circulation would greatly enhance momentum and mass transfer away from the storm center and aid in rapid storm development. The degree of transfer created by this process would, of course, determine the speed at which the storm developed. Since Anna intensified rapidly it seems that such a process was in operation here.

The phenomenon of the annular ring frequently mentioned in studies of the mature hurricane could not be clearly identified as a result of peripheral storm subsidence in the case of Hurricane Anna. The clear zone on the forward half of the storm seemed to be associated with dry air advected around the front of the storm from higher latitudes with flow instabilities creating the cloud bands present. This concept is supported to some extent by the development of a warm tongue in the radiation data in front of the storm as the circulation of the system increased. In addition, aircraft observations showed well-defined clear bands alternating with cloud bands from well behind the cirrus shield edge to well beyond the edge with thin middle-cloud wisps occurring over much of the clear ocean area in the vicinity of the cirrus rim.

The outer shear line which preceded the storm did not become closely associated with the cloud boundary until the storm had passed maximum intensity. Prior to that time it was as far as 13 degrees from the storm center when the storm was at hurricane intensity. The outer shear line did have an associated warm and dry area below it suggesting that if it had been coincident with the cloud edge as in other studies a good association between the cirrus rim and deep drying would have been found.

Storm decay commenced about the time the southern edge of the cirrus shield passed over land early on July 23. The actual storm center just grazed the northern coast of Honduras late on July 23 and finally went aground about midday on July 24 on the British Honduras coast. By July 25 the cloud features associated with the decayed storm consisted mainly of a few convection centers associated with the tropical depression and an overlay of thin cirrus. What little remained of the storm moved up the Mexican Gulf coast with all traces of the associated cloud activity lost by July 27.

6. Conclusions and Recommendations

Hurricane Anna took seven days to reach maximum intensity from the time it started to intensify from its mid-Atlantic easterly wave stage. Initially, the wave had two separate cloud areas and this form was maintained until just before hurricane intensity was reached. It is proposed that warm core creation occurred at approximately the time the cirrus canopy covered the storm system and that the period of rapid intensification followed. The storm circulation seemed to develop from aloft and work downward as indicated by both the cloud and time cross-section features examined. The anticyclone aloft was present before the storm began its most rapid intensification and the entire wave intensification apparently occurred under a tropical high. Rapid storm intensification seemed to coincide with the appearance of major spiral bands in the cloud field. The spiral bands detected in the developing hurricane and which later formed an almost complete convection ring about the storm probably contributed to hurricane intensification as suggested by Fujita. The bands that first became apparent seemed to form an inner convection ring while an outer convection band seemed to develop about the time the storm reached maximum intensity. The clear area between the inner convection bands and the inner cirrus shield and the outer convection band observed in some NIMBUS pictures of typhoons was not present, but this could be a feature of individual storm mechanics rather than general storm organization.

As the high cloud shield developed, a warm tongue of air appeared in front of the storm and to some degree around the southern end of the cloud shield. In view of the vertical cross-sections through the area in question, it seems probable that the warm tongue was associated with the cirrus rim to account for the clear moat about the storm at maximum intensity.

The strong shear line that various authors have found at the leading edge of the cirrus cover occurred only in the final stages of Hurricane Anna. This suggests that

when the storm is in the more southern latitudes the association between the outer shear line and the cirrus shield, especially in the forward quadrant, could be considerably different than in the cases of storms in more northern latitudes. The effect of the low level drying due to advection on storm intensity is doubtful, although in the case of Hurricane Anna one is tempted to say it contributes to the decay of the storm while over water.

Observation of storm development at a later time when a larger amount of supporting data are available in addition to present satellite information will aid greatly in constructing a model of storm development. Until that time, the question of dry air advection versus high level subsidence as a cause of the clear ring and time of warm core creation with respect to cloud cover will remain largely speculative. The study of tropical storms will be greatly aided when individual storms can be followed for long periods of time. Studies of individual storms could then be compared with the general studies now available to yield a better understanding of storm development. Following individual storms through their life cycle, moreover, will greatly aid in the determination of the relation between the outer and inner convective bands on storm intensification.

REFERENCES

Allison, L. J. and G. W. Nicholas, 1964: Examples of the Meteorological Capacity of the Nimbus Satellite. Observations from the Nimbus I Meteorological Satellite. NASA SP 89, 61-89.

Arnold, J. E., 1966: Easterly wave activity over Africa and in the Atlantic with a note on the Intertropical Convergence Zone during early July, 1961, SMRP Rep. 65.

Erickson, C. O., 1963: An incipient hurricane near the West African coast. Mon. Wea. Rev., 91, 61-68.

Fett, R. W., 1964: Some characteristics of the formative stage of typhoon development; A satellite study. United States Weather Bureau Monograph, 22 pp.

_____, 1964: Aspects of hurricane structure: New model considerations suggested by TIROS and Project Mercury observations. Mon. Wea. Rev. 92, 43-60.

Fritz, Sigmund, 1962: Satellite pictures and the origin of Hurricane Anna. Mon. Wea. Rev. 90, 507-513.

Fujita, T. and J. Arnold, 1963: Detection of hurricanes using TIROS infrared data. Proceedings of the Symposium on Tropical Meteorology, New Zealand Meteorological Service, 582-589.

Fujita, T; T. Izawa, K. Watanabe, and I. Imai, 1966: A model of typhoons accompanied by inner and outer rainbands. SMRP Rep. 60.

Merritt, E. S., 1965: Analysis and forecasting techniques utilizing meteorological satellite data. Aracon Geophysics Co. Final Report (Part A) Contract No. 189(188)-58014A.

Reap, R. M., 1966: Preliminary investigation of peripheral subsidence associated with hurricane outflow. SMRP Rep. 63.

Riehl, H., 1954: Tropical Meteorology, McGraw Hill, New York, N. Y., 392 pp.

Sadler, J. C., 1964: Tropical cyclones of the eastern North Pacific as revealed by TIROS observations. J. of Appl. Meteor. 3, 4, 347-366.

Shiroma, M., and J. Sadler, 1965: TIROS observations of typhoon formation. Scientific Rep. 1, Contract No. AF19(628)-3860, University of Hawaii.

U.W. Fleet Weather Facility, 1962: Annual tropical storm report 1961. OPNAV Report 3140-9, 11-17 Part II; 11-37, Annex A.

Yanai, M., 1961: A detailed analysis of typhoon formation. J. of Met. Soc. of Japan, 39, 175-214.

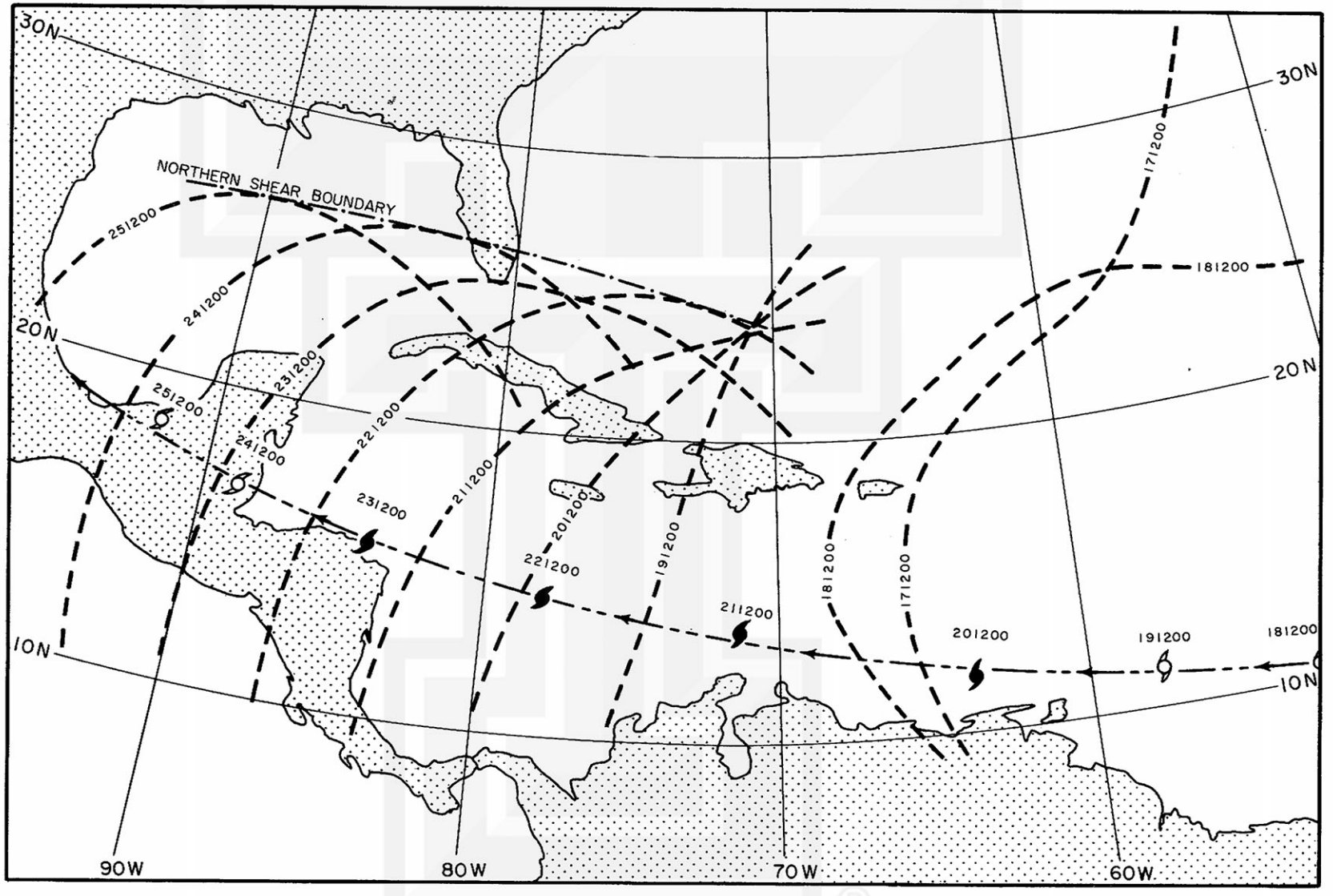

Fig. 1. The relationship between the outer shear line and storm location during the life of Hurricane Anna. Note that the shear line is farthest from the storm early in the life of the storm, with the distance decreasing with storm age.

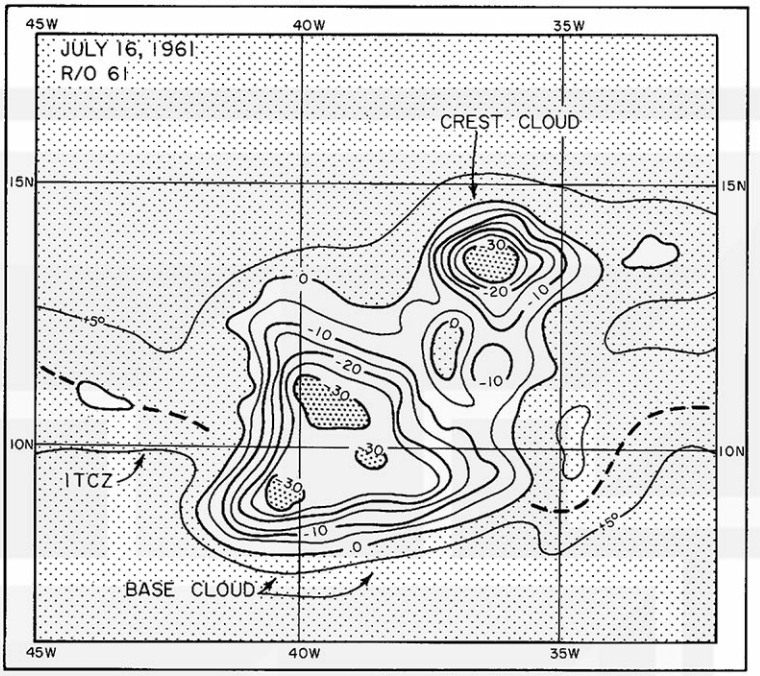

Fig. 2. Radiation map (8-12μ) for July 16, 1961 (1523 GMT 60 R/O 61) of the disturbance which produced Hurricane Anna. The system is bimodal at this time and connects to the main cloud band associated with the ITCZ.

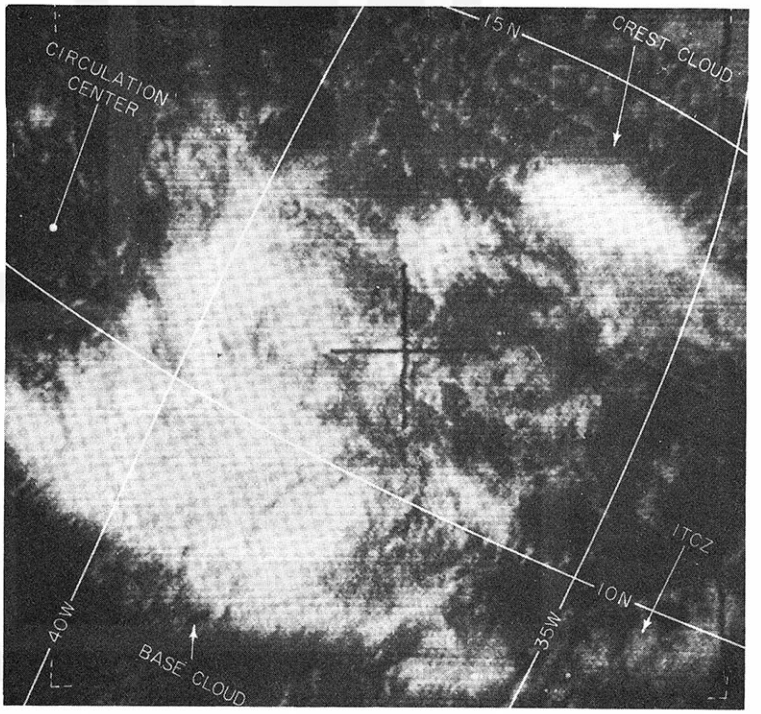

Fig. 3. Photograph of the Anna-producing disturbance on July 16 (1520 GMT R/O 61). The wave axis is believed to be just west of the main cloud mass.

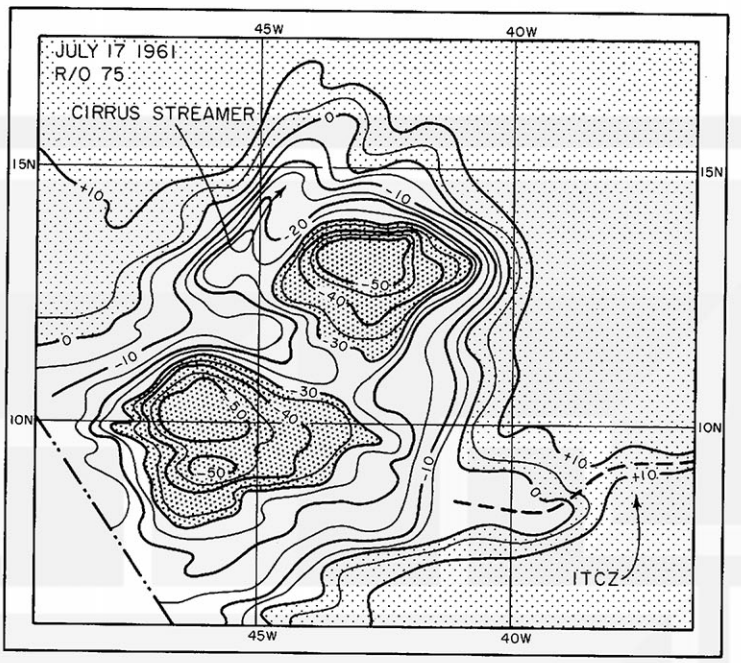

Fig. 4. Radiation map (8-12 μ) for July 17, 1961 (1447 GMT R/O 75) of the disturbance which produced Hurricane Anna. At this time the wave is in its second day of active intensification.

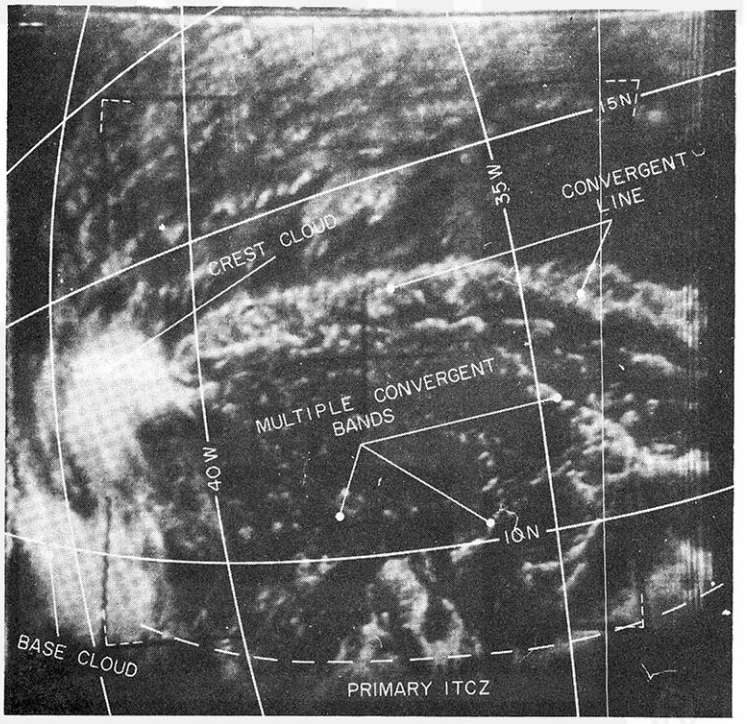

Fig. 5. Photograph of the Anna-producing disturbance on July 17, 1961 (1450 GMT R/O 75). Note the long cloud trail from the crest cloud. The main ITCZ cloud band passing through the base cloud is faintly visible on the southern boundary of the picture.

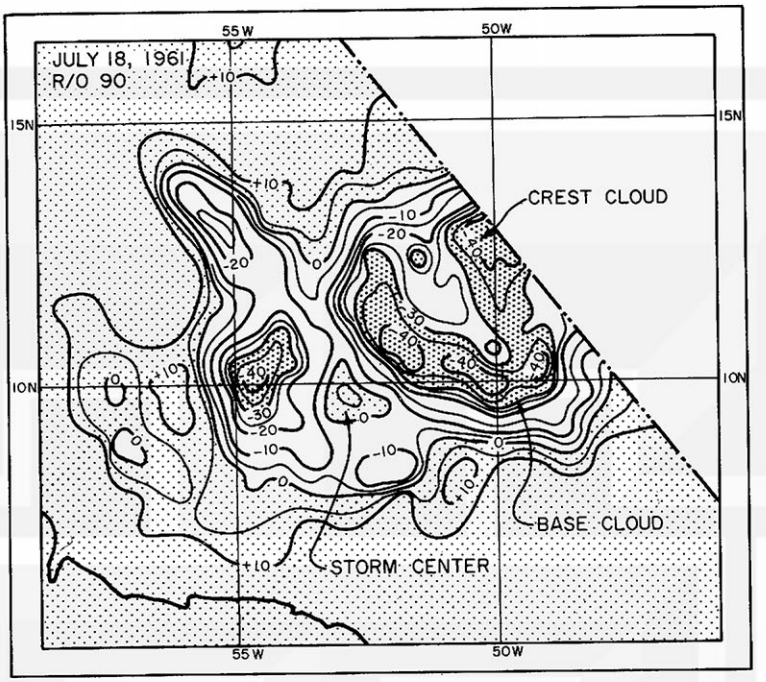

Fig. 6. Radiation map (8-12μ) for July 18, 1961 (1552 GMT R/O 90) showing the developing disturbance. Strong convection activity appears to have begun on the western side of the circulation center or wave axis of the storm.

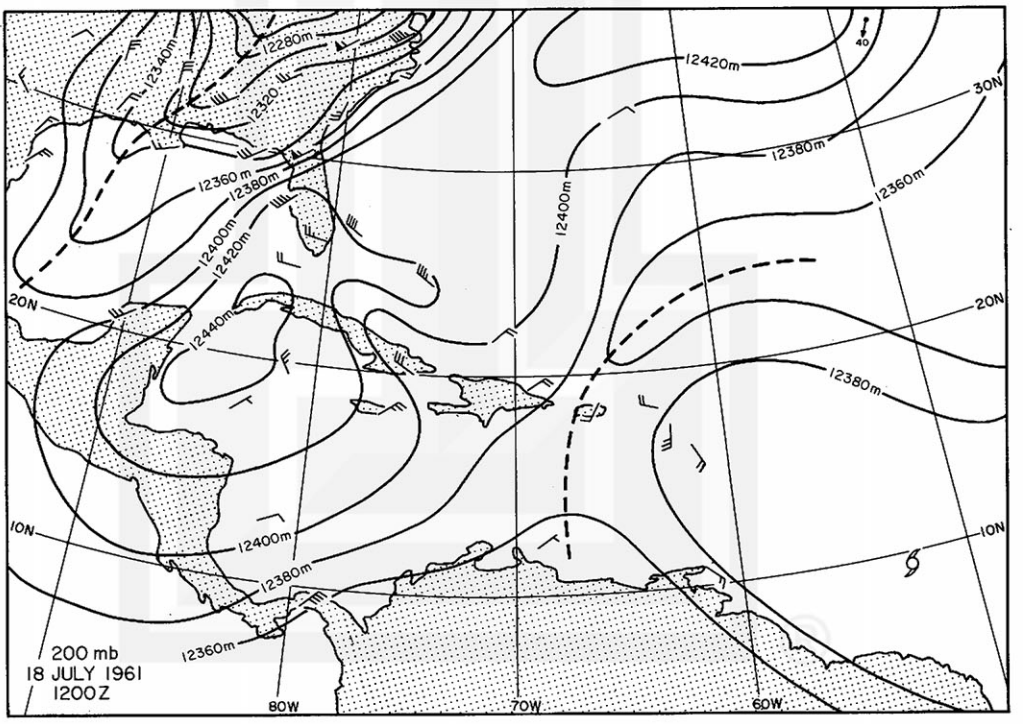

Fig. 7. 200 mb chart for 1200 GMT July 18, 1961. The large tropical high over the storm has sheared off the southern end of an eastward-traveling subtropical trough and is pushing it westward.

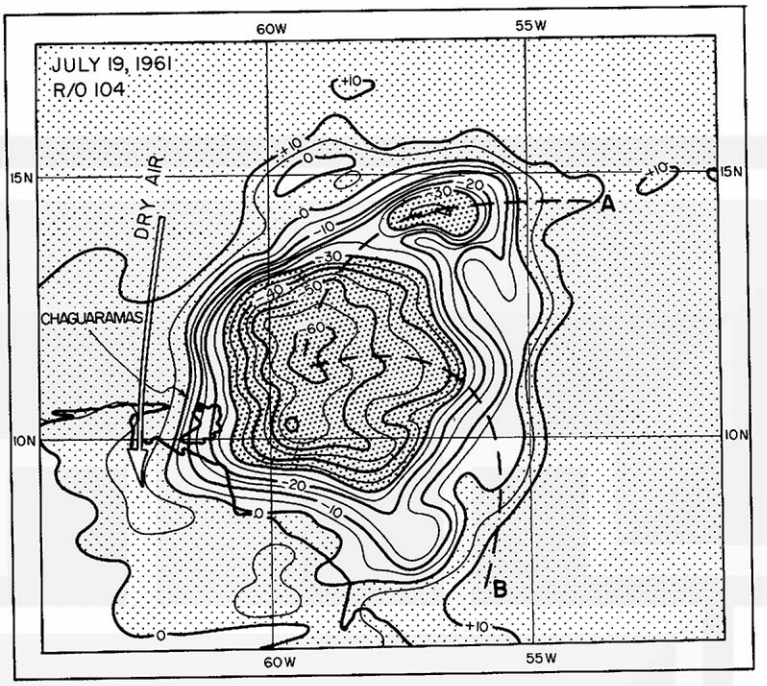

Fig. 8. Radiation map (8-12 μ) for July 19, 1961 (1336 GMT R/O 103). The storm center, while still below hurricane intensity, has become covered with cirrus with the crest cloud remaining isolated. Note the warm tongue of air extending the forward half of the storm.

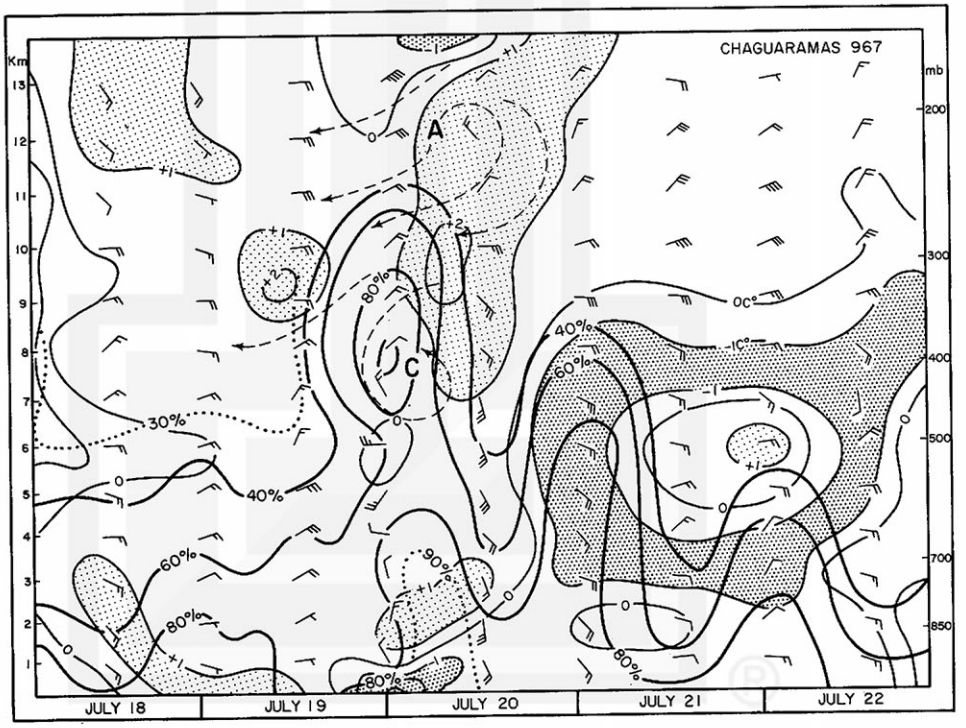

Fig. 9. Time cross-section for Chaguaramas from July 18-22, 1961, showing winds, temperature deviations from a 14 day mean (thin solid lines) surrounding the time of the cross section (00 and 1200 GMT observations treated independently) and relative humidity contours (heavy solid lines). Note the warm core and circulation center above 400 mb.

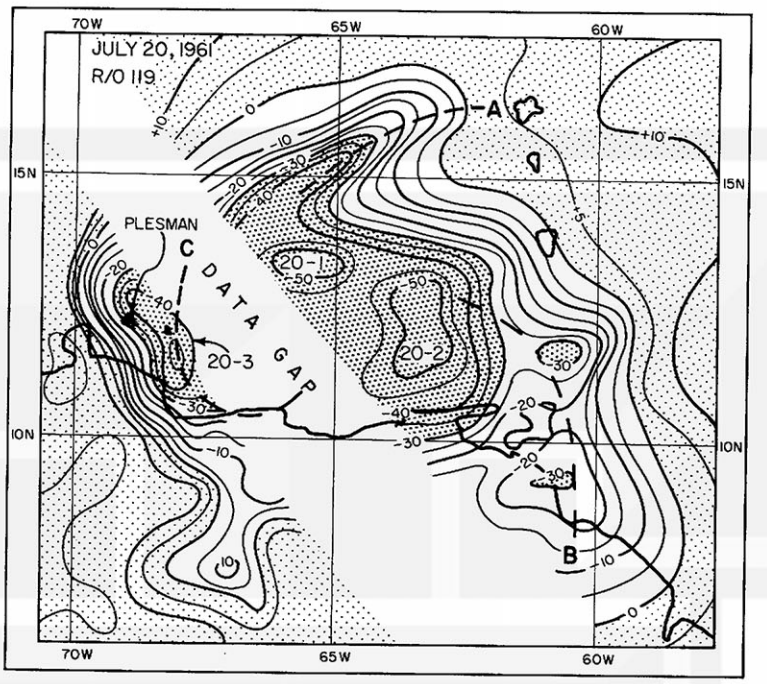

Fig. 10. Radiation map (8-12μ) of Hurricane Anna on July 20, 1961 (made by combining orbits R/O 118 at 1441 GMT and R/O 119 at 1627 GMT) immediately after the storm had reached hurricane intensity.

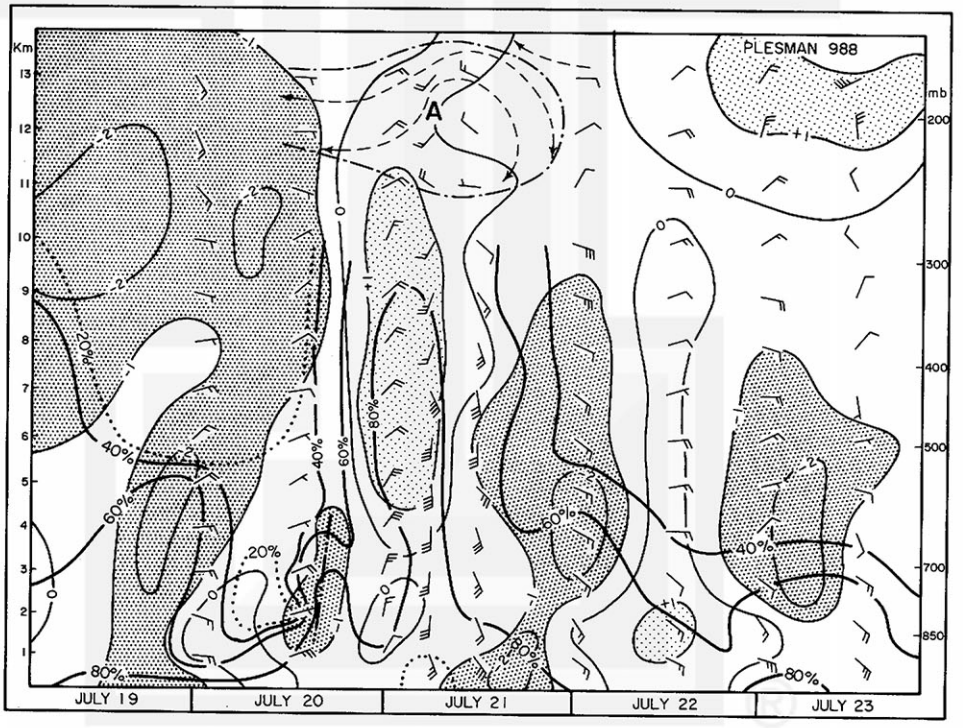

Fig. 11. Time cross-section for Plesman from July 19-23, 1961, showing winds, temperature deviations from a 14 day mean surrounding the time of the cross section (00 and 1200 GMT observations treated independently) and relative humidity contours. Note the well developed anticyclone at 200 mb and the expanded warm core. The cold-core line immediately in front of the storm corresponds well with the convection band observed in the satellite photograph on July 20.

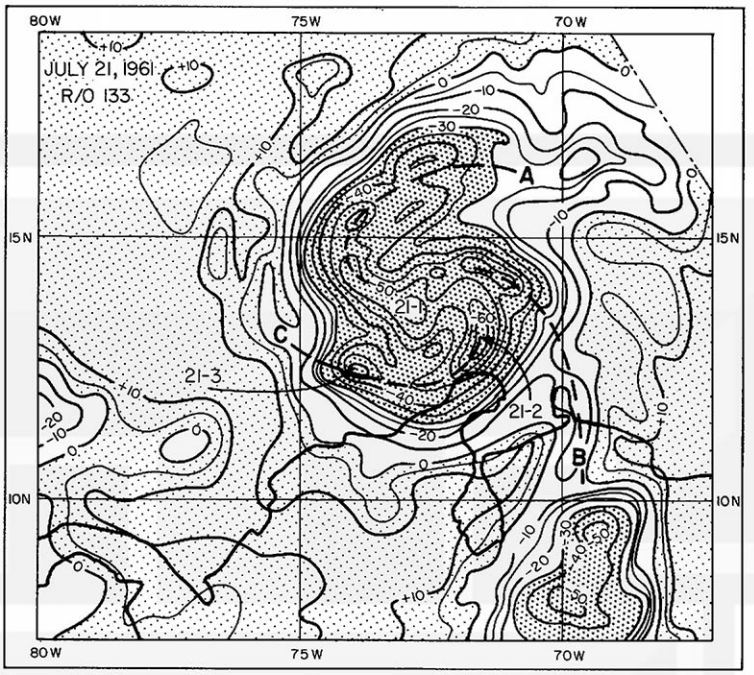

Fig. 12. Radiation map (8-12 μ) of Hurricane Anna on July 21 (1545 GMT R/O 133) showing the well developed spiral bands in the cloud top. Note that the north band overlays the crest cloud that existed on earlier stages.

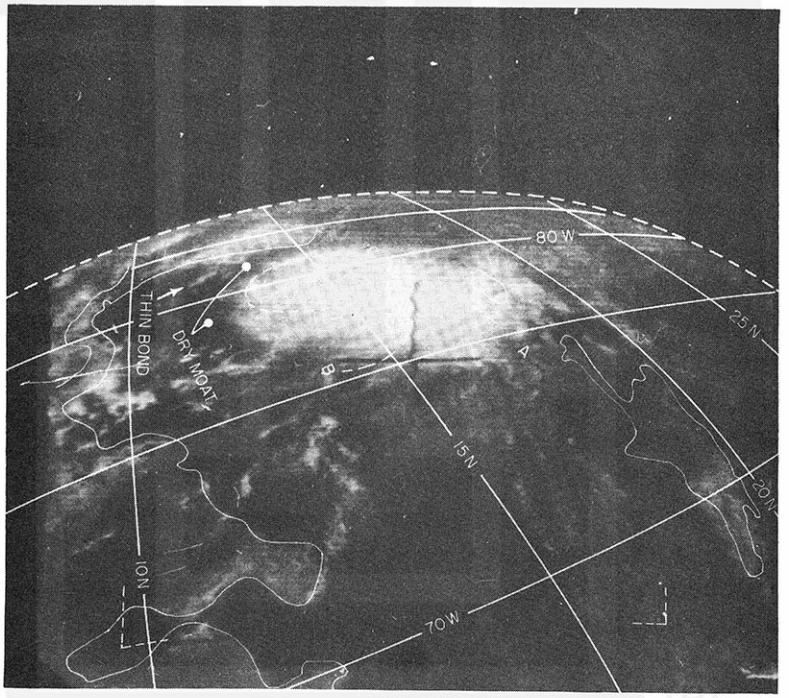

Fig. 13. Photograph of Hurricane Anna on July 22, 1961 (1513 GMT R/O 147) at the time the storm was at maximum intensity. The cirrus canopy over the storm is an isolated cloud mass which has expanded over the earlier cloud bands. Small bright cloud masses are located in the forward half of the cirrus rim, and are possibly the tops of convection cells in the outer convection band.

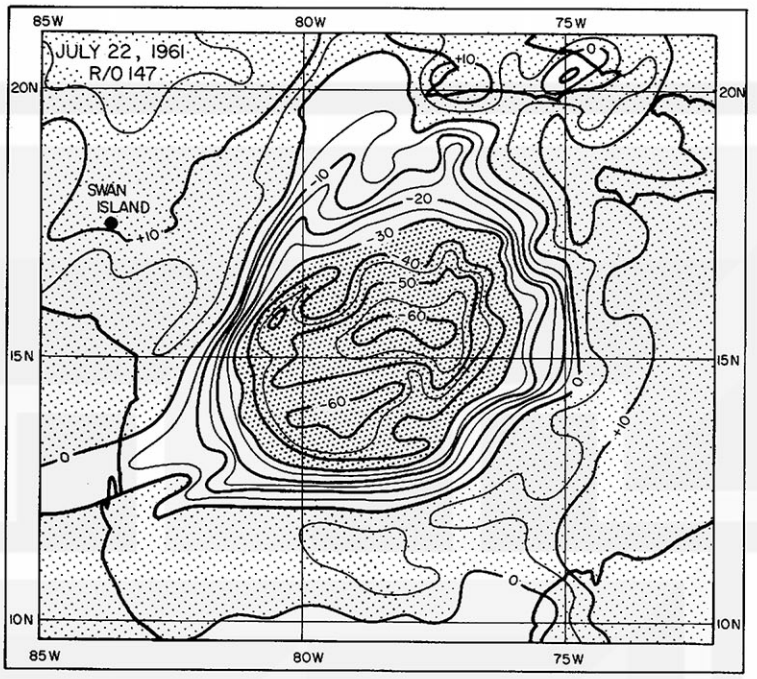

Fig. 14. Radiation map (8-12μ) of Hurricane Anna on July 22, 1961 (1516 GMT R/O 147). Note that there is some elongation of the cloud features on the western edge because of its proximity to the scan boundary.

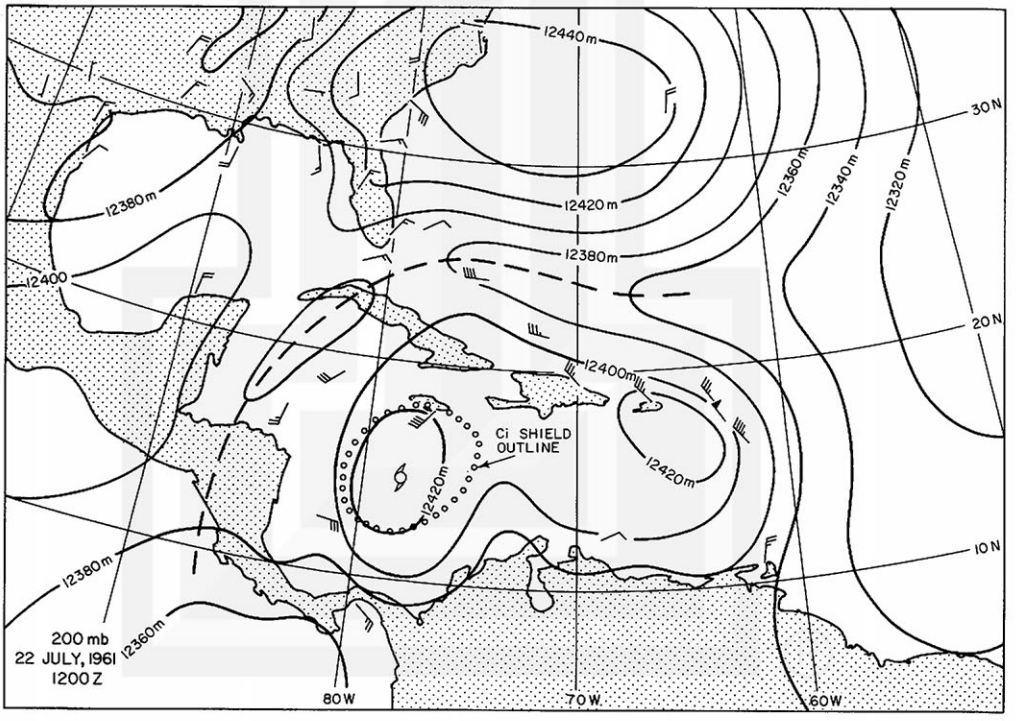

Fig. 15. 200 mb analysis for 1200 GMT July 22, 1961. The dotted circle about the hurricane center is the extent of the cirrus shield at 1513 GMT July 22, 1961.

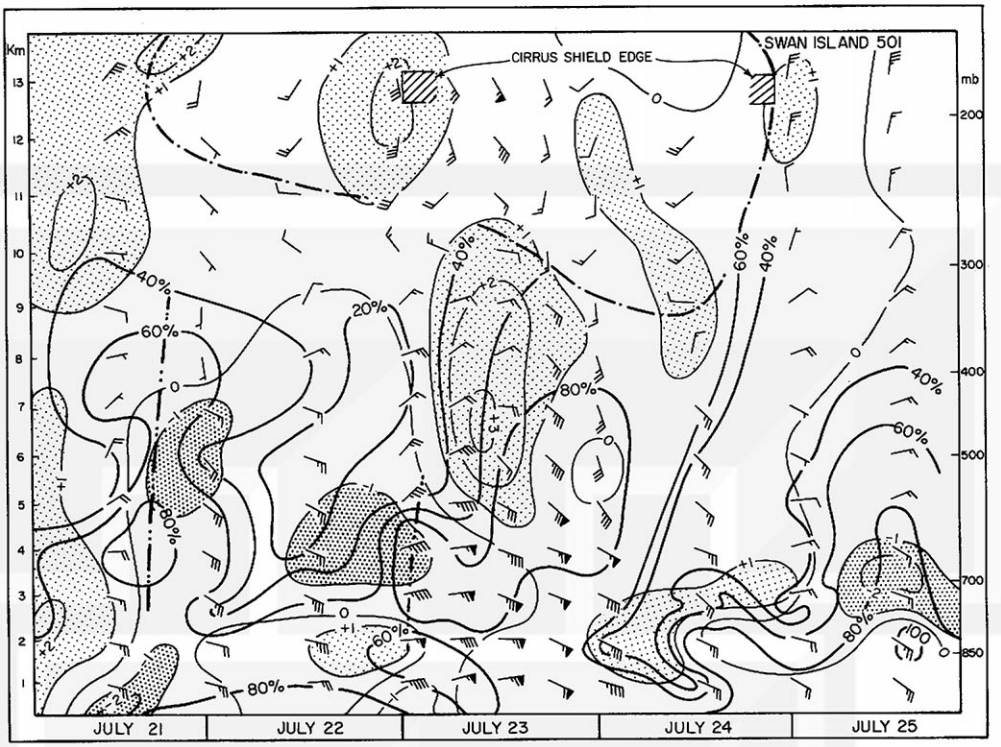

Fig. 16. Time cross-section for Swan Island from July 21-25, 1961 showing winds, temperature deviations from a 14 day mean surrounding the time of the cross section (00 and 1200 GMT observations treated independently) and relative humidity contours. Note the small warm areas at the cirrus shield edge. In addition to the outer shear line at 200 mb, two discontinuities are present below 400 mb. The outer line occurs below the upper-level shear line and the inner line coincides closely with the cirrus edge.

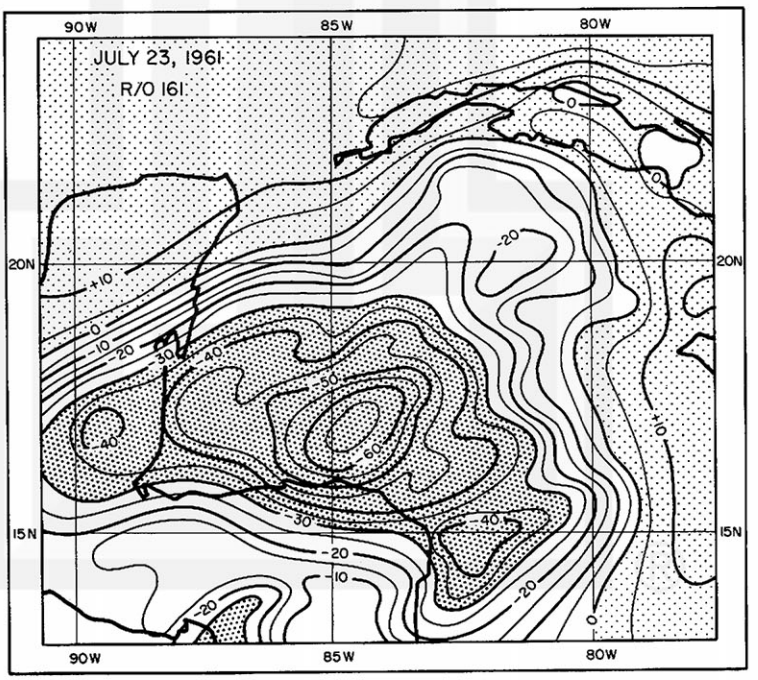

Fig. 17. Radiation map of Hurricane Anna for July 23, 1961 (1533 GMT R/O 161). The extreme east-west elongation on the western boundary is partially due to its proximity to the scan horizon.

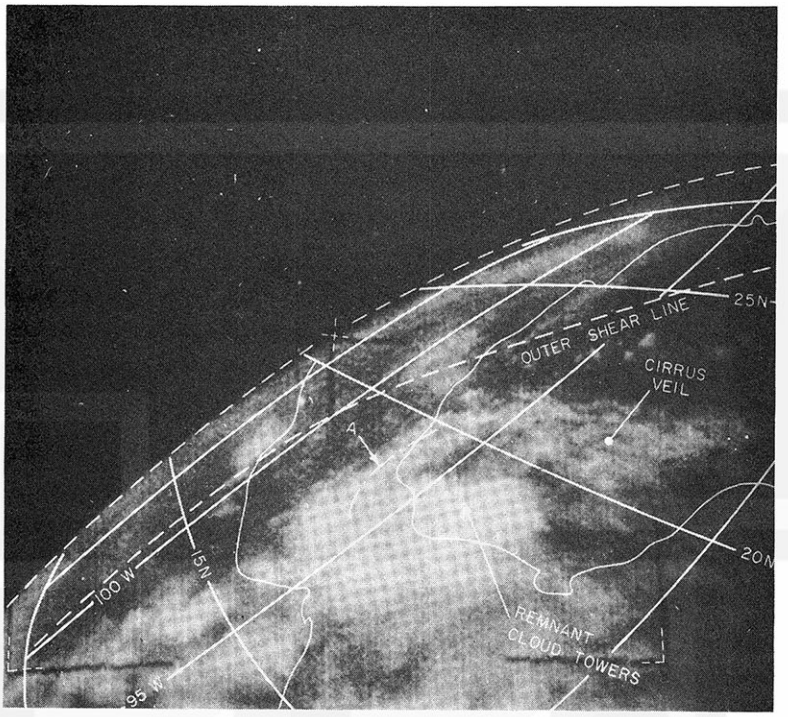

Fig. 18. Photograph of the decayed stage of the hurricane on July 25, 1961 (1505 GMT R/O 190). Note the cirrus coverage in relation to the outer shear line.

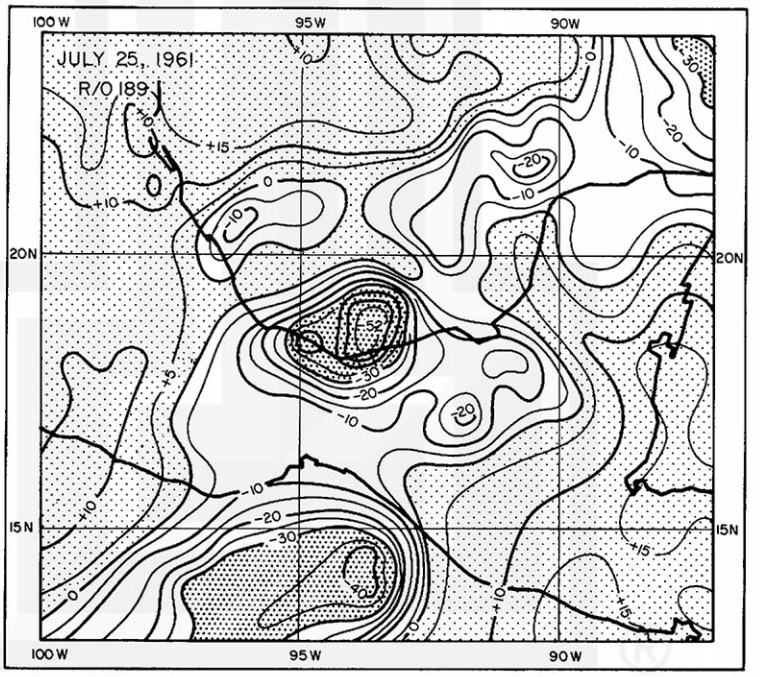

Fig. 19. Radiation map (8-12μ) of the decayed stage of Hurricane Anna on July 25, 1961 (1505 GMT R/O 190). The large cirrus shield has begun to dissolve leaving an isolated cold cloud-top over the surface depression.

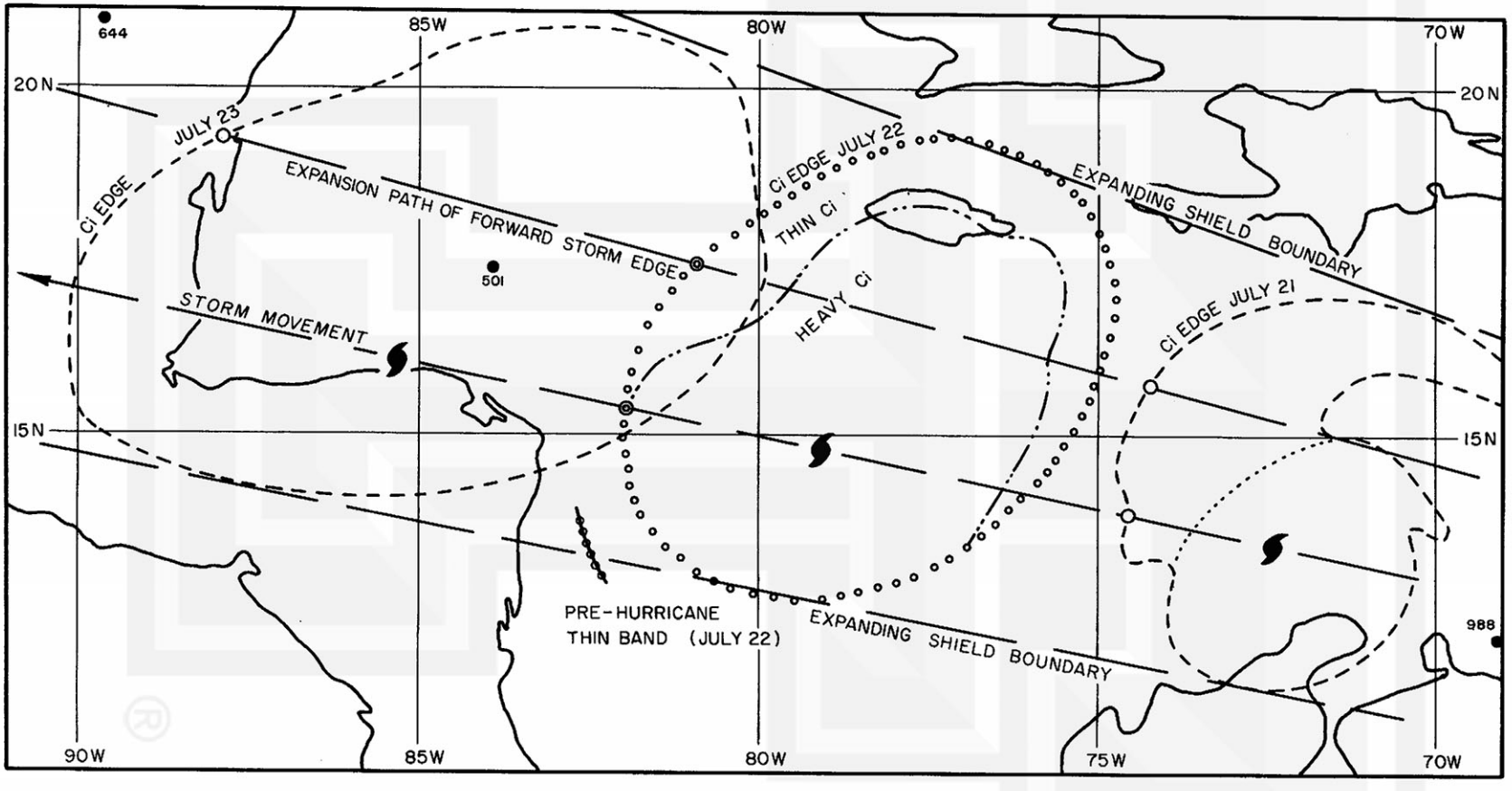

Fig. 20. Expansion of the cirrus shield over Hurricane Anna from July 21 through July 23 from photographic information. Note that the main expansion of the shield was over the northern cloud band and along the axis of maximum winds at 200 mb.

APPENDIX A

Radiation maps of the early wave stage of Hurricane Anna off the coast of Africa.

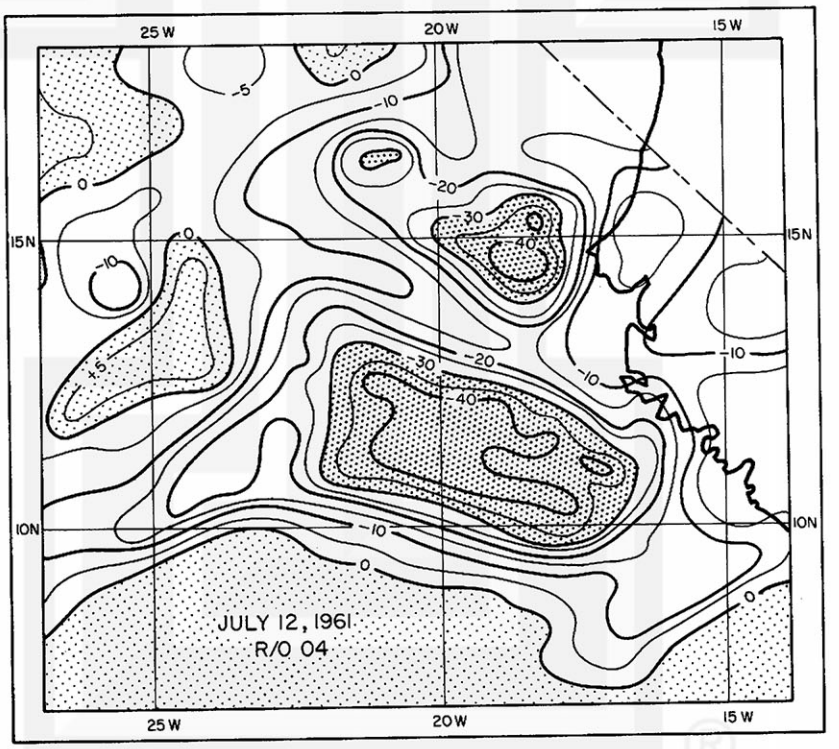

Fig. A1. Radiation map (8-12 μ) of the Anna wave on July 12, 1961 (1608 GMT R/O 04). The wave had crossed into the Atlantic from Africa on the previous day after crossing central and western Africa.

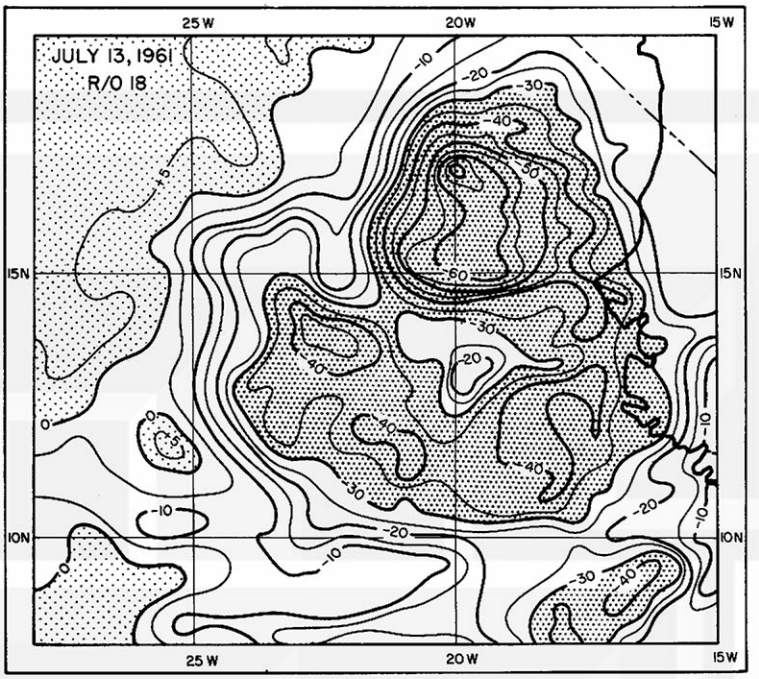

Fig. A2. Radiation map (8-12 μ) of the Anna wave on July 13, 1961 (1530 GMT R/O 18). Note the large increase in cloud cover believed to have been caused by the wave coincidence with a subtropical trough.

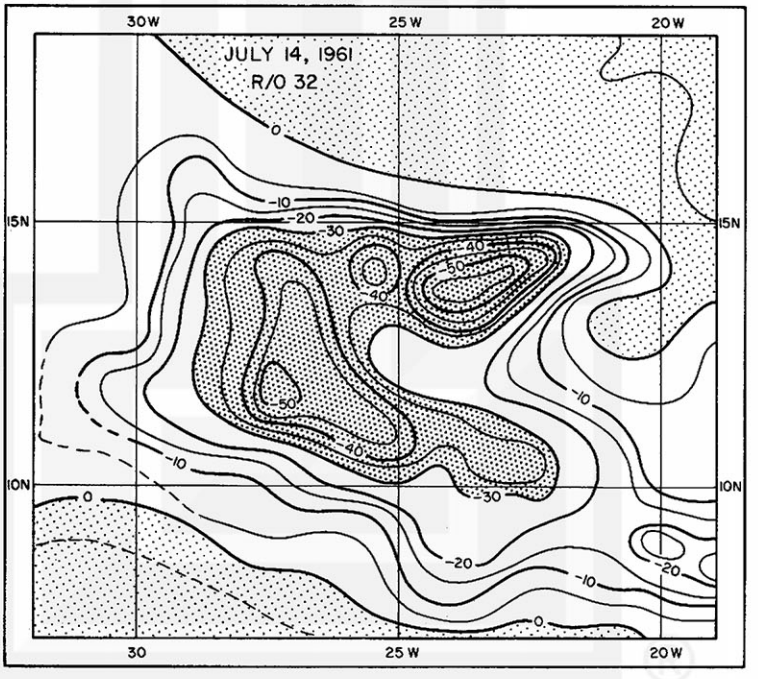

Fig. A3. Radiation map (8-12 μ) of the Anna wave on July 14, 1961 (1454 GMT R/O 32). Westward movement of the wave has been accompanied by a decrease in cloud activity.

APPENDIX B

Sequential photographs of the developing and mature Hurricane Anna.

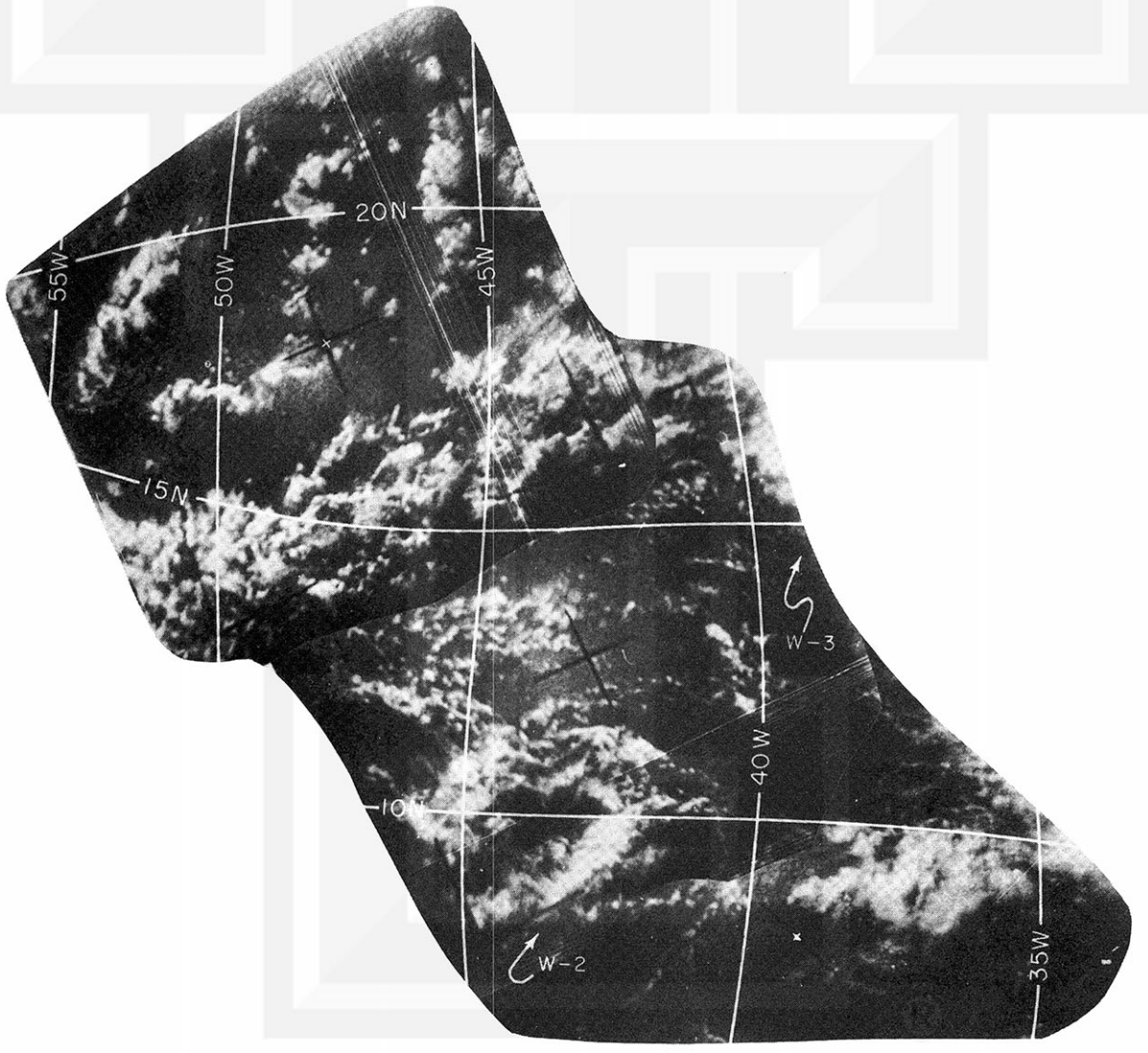

Fig. B1. Mosaic of the ITCZ on July 15, 1961 at about 1557 GMT. The cloud mass at 10N and 44W is, from continuity, approximately the position the Anna wave should occupy.

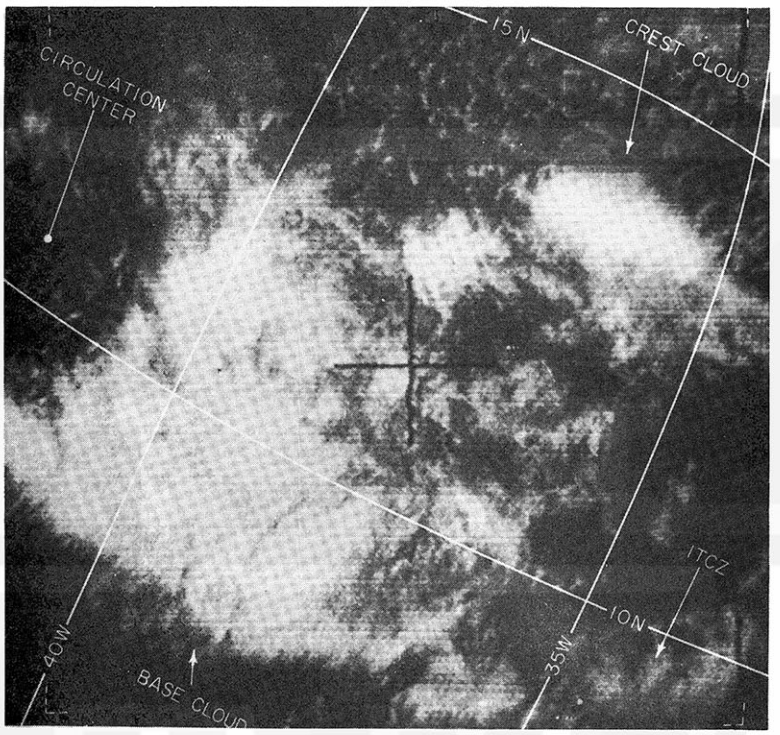

Fig. B2. July 16, 1961 photograph of the Anna wave (1523 GMT R/O 61).

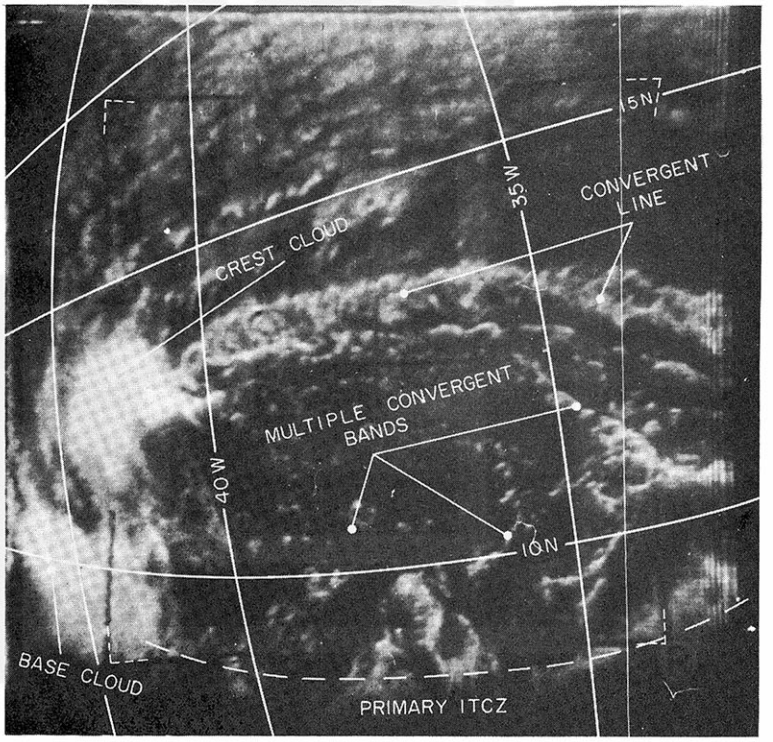

Fig. B3. July 17, 1961 photograph of the Anna wave (1450 GMT R/O 75).

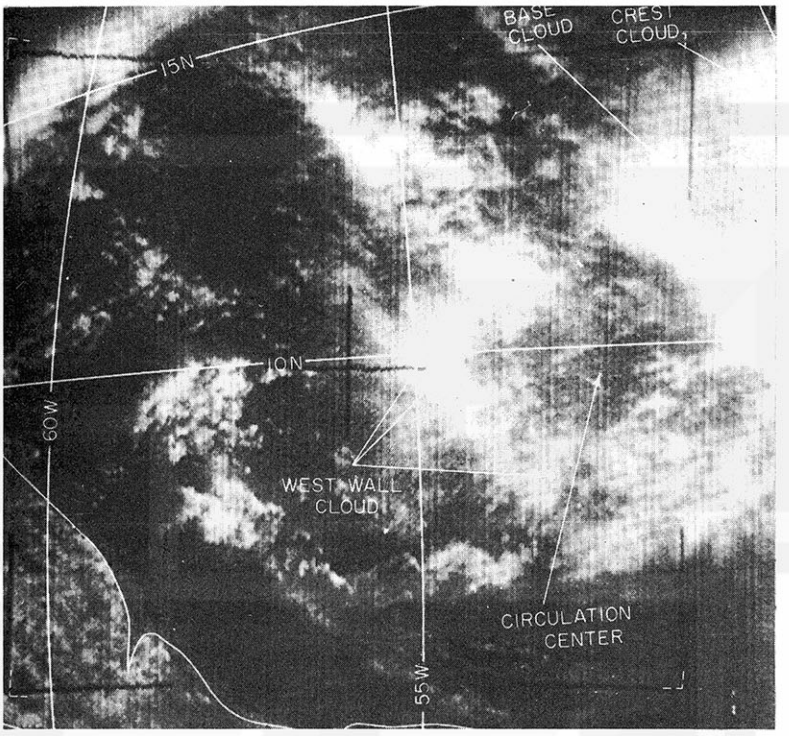

Fig. B4. July 18, 1961 photograph of the Anna wave (1555 GMT R/O 90).

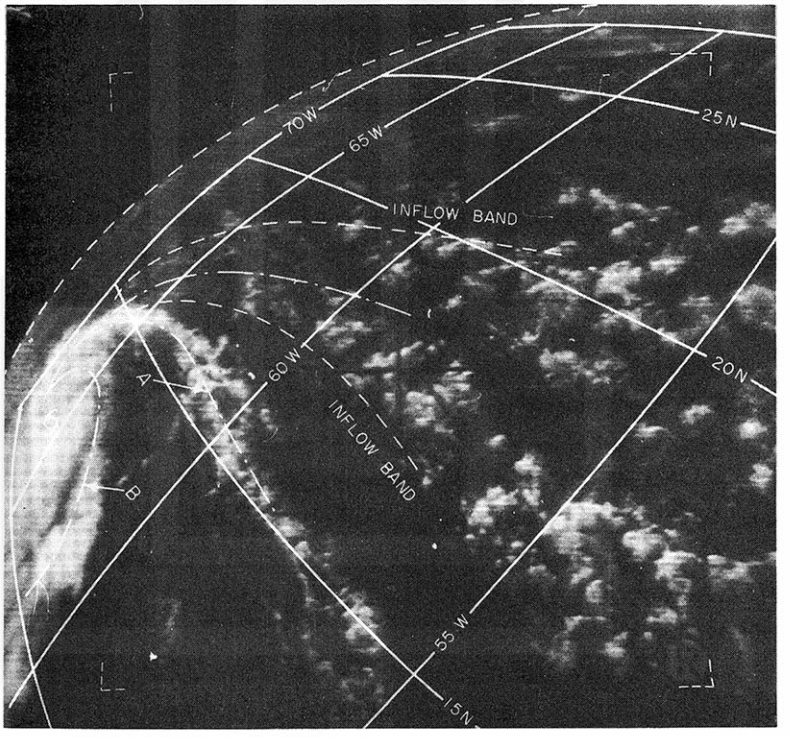

Fig. B5. July 20, 1961 photograph of Hurricane Anna (1619 GMT R/O 118).

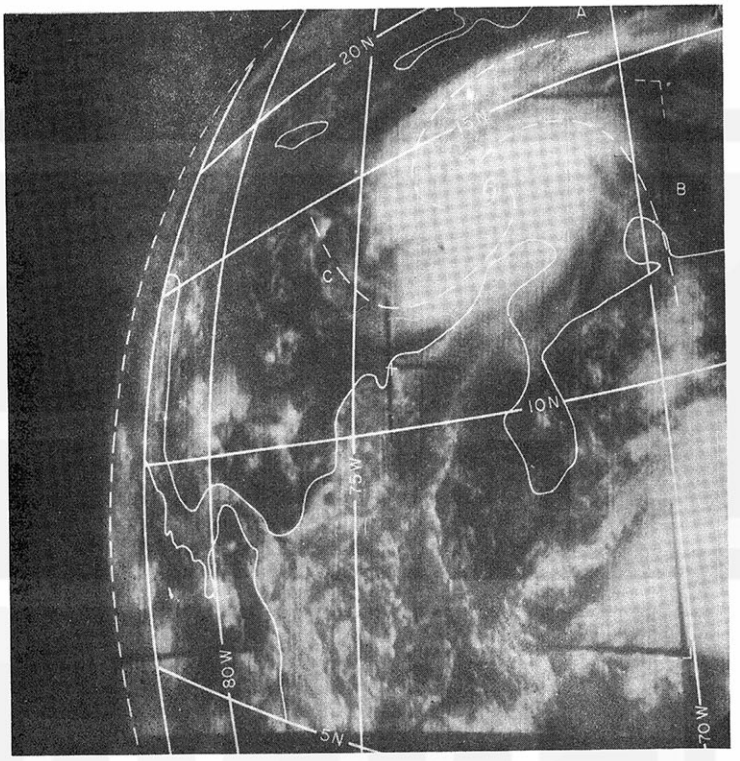

Fig. B6. July 21, 1961 photograph of Hurricane Anna (1450 GMT R/O 133).

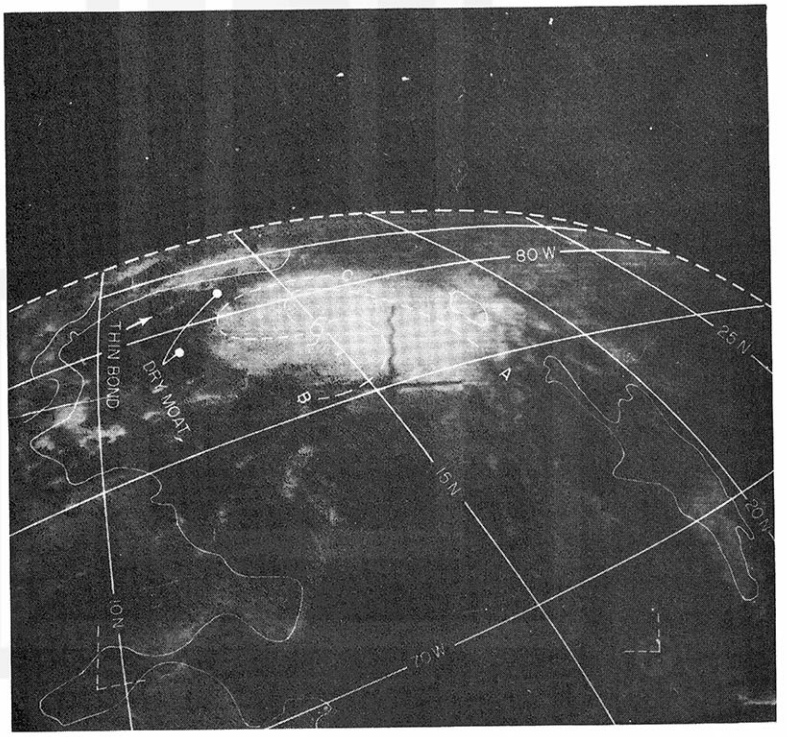

Fig. B7. July 22, 1961 photograph of Hurricane Anna (1513 GMT R/O 147).

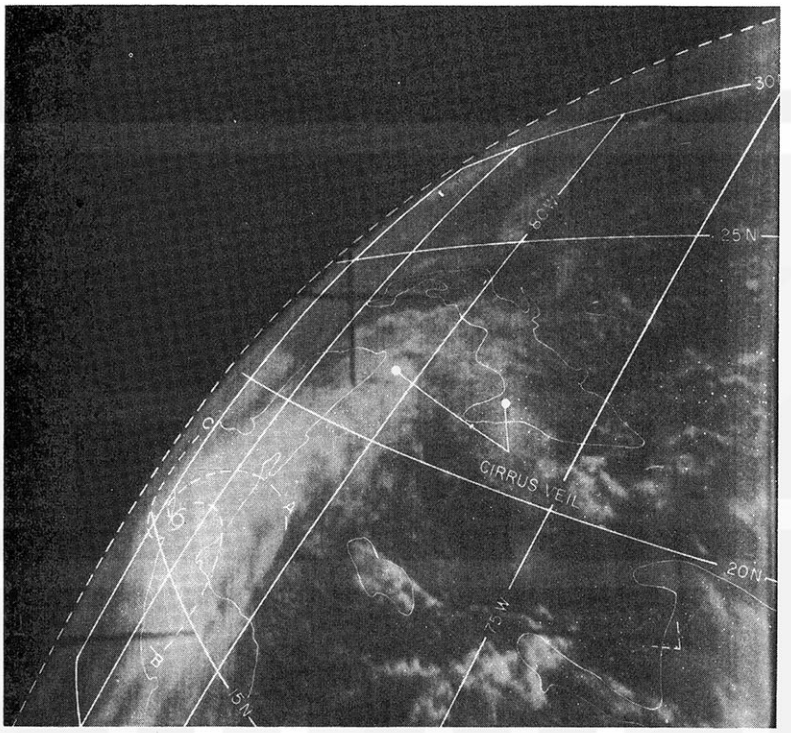

Fig. B8. July 23, 1961 photograph of Hurricane Anna (1430 GMT R/O 161).

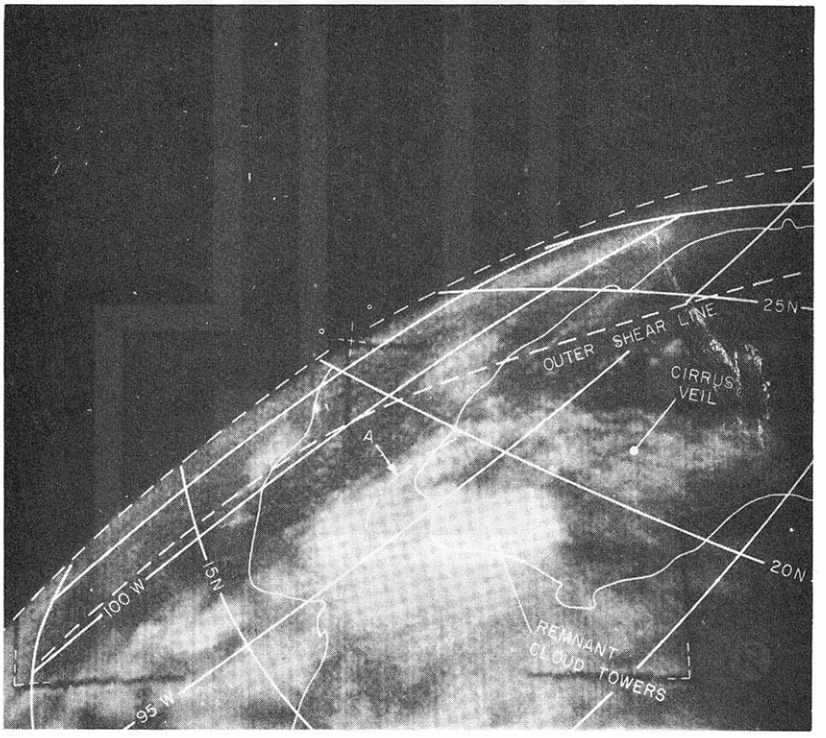

Fig. B9. July 25, 1961 photograph of the remnants of Hurricane Anna (1505 GMT R/O 189).

MESOMETEOROLOGY PROJECT - - - RESEARCH PAPERS

(Continued from front cover)

42. A Study of Factors Contributing to Dissipation of Energy in a Developing Cumulonimbus - Rodger A. Brown and Tetsuya Fujita
43. A Program for Computer Gridding of Satellite Photographs for Mesoscale Research - William D. Bonner
44. Comparison of Grassland Surface Temperatures Measured by TIROS VII and Airborne Radiometers under Clear Sky and Cirriform Cloud Conditions - Ronald M. Reap
45. Death Valley Temperature Analysis Utilizing Nimbus I Infrared Data and Ground-Based Measurements - Ronald M. Reap and Tetsuya Fujita
46. On the "Thunderstorm-High Controversy" - Rodger A. Brown
47. Application of Precise Fujita Method on Nimbus I Photo Gridding - Lt. Cmd. Ruben Nasta
48. A Proposed Method of Estimating Cloud-top Temperature, Cloud Cover, and Emissivity and Whiteness of Clouds from Short- and Long-wave Radiation Data Obtained by TIROS Scanning Radiometers - T. Fujita and H. Grandoso
49. Aerial Survey of the Palm Sunday Tornadoes of April 11, 1965 - Tetsuya Fujita
50. Early Stage of Tornado Development as Revealed by Satellite Photographs - Tetsuya Fujita
51. Features and Motions of Radar Echoes on Palm Sunday, 1965 - D. L. Bradbury and Tetsuya Fujita
52. Stability and Differential Advection Associated with Tornado Development - Tetsuya Fujita and Dorothy L. Bradbury
53. Estimated Wind Speeds of the Palm Sunday Tornadoes - Tetsuya Fujita
54. On the Determination of Exchange Coefficients: Part II - Rotating and Nonrotating Convective Currents - Rodger A. Brown
55. Satellite Meteorological Study of Evaporation and Cloud Formation over the Western Pacific under the Influence of the Winter Monsoon - K. Tsuchiya and T. Fujita
56. A Proposed Mechanism of Snowstorm Mesojet over Japan under the Influence of the Winter Monsoon - T. Fujita and K. Tsuchiya
57. Some Effects of Lake Michigan upon Squall Lines and Summertime Convection - Walter A. Lyons
58. Angular Dependence of Reflection from Stratiform Clouds as Measured by TIROS IV Scanning Radiometers - A. Rabbe
59. Use of Wet-beam Doppler Winds in the Determination of the Vertical Velocity of Raindrops inside Hurricane Rainbands - T. Fujita, P. Black and A. Loesch
60. A Model of Typhoons Accompanied by Inner and Outer Rainbands - Tetsuya Fujita, Tatsuo Izawa, Kazuo Watanabe, and Ichiro Imai

MESOMETEOROLOGY PROJECT - - - RESEARCH PAPERS

(Continued from inside back cover)

61. Three-Dimensional Growth Characteristics of an Orographic Thunderstorm System - Rodger A. Brown.

62. Split of a Thunderstorm into Anticyclonic and Cyclonic Storms and their Motion as Determined from Numerical Model Experiments - Tetsuya Fujita and Hector Grandoso.

63. Preliminary Investigation of Peripheral Subsidence Associated with Hurricane Outflow - Ronald M. Reap.